

TUMSAT-OACIS Repository - Tokyo

University of Marine Science and Technology

(東京海洋大学)

Modeling of ohmic heating of solid food with
non-uniform electric properties

メタデータ	言語: eng 出版者: 公開日: 2017-02-15 キーワード (Ja): キーワード (En): 作成者: 郭, 雯 メールアドレス: 所属:
URL	https://oacis.repo.nii.ac.jp/records/1371

Master's Thesis

**Modeling of Ohmic Heating of Solid
Food with Non-uniform Electric
Properties**

September 2014

Graduate School of Marine Science and Technology
Tokyo University of Marine Science and Technology
Master's Course of Food Science and Technology

Guo Wen

[修士]

修士学位論文内容要旨
Abstract

専攻 Major	食機能保全科学 Food Science and Technology	氏名 Name	郭 雯 Guo Wen
論文題目 Title	不均一電気特性を有する固体食品の通電加熱のモデル化 Modeling of Ohmic heating of solid food with non-uniform electric properties		

【Background and Objective】

Being a novel energy-efficient method, ohmic heating (OH) has attracted the interest of food industry recently. Since the main critical factor in thermal processes is the thermal history and the temperature distribution during OH requires special consideration of the current knowledge, the non-uniform temperature distribution inside heterogeneous food after OH indicates the importance of investigation on the thermal behavior of complex system. However, there is not a lot of data available for heterogeneous food especially for the solid composite food. Therefore, modeling of the thermal behavior of composite food with various electric conductivities during OH has been a challenge. In this study, the temperature distributions and profiles of four typical solid composite food systems designed for the parallel and series model and two typical surrounding-cases: pure-inside-salt model and salt-inside-pure model were investigated undergoing OH. And a new method of predicting the heat generation inside the food during OH based on electromagnetic field analysis by Maxwell's equations was proposed instead of Joule's law.

【Materials and Methods】

Electric conductivity measurement

Mashed potato and mashed potato with 1wt % sodium chloride (water content of both were 80wt %) were used as the pseudo food samples in this study. Electric conductivity, σ ($S m^{-1}$) of the two materials, which was the important parameter used in simulating, could be calculated from the impedances that were measured in water bath by LCR meter (HiTESTER3532-50, HIOKI Co. Ltd., Japan) from 20 to 80 °C, every 5 °C.

Investigation of temperature distribution undergoing OH

Temperature distributions of four filling patterns after OH were investigated. And during heating, an OH machine (FJB-55, Frontier Engineering Co. Ltd., Japan) was applied for supplying the alternating current (50V, 20 kHz). After OH of certain time, the thermal pictures of the cross-section were captured by an infrared thermal camera (TH7102WV, NEC San-ei Instruments, Ltd., Japan) to verify the estimations.

Temperature analysis by 3D finite element computational model

Two commercial finite methods based software packages, FEMAP (V10.2, Siemens PLM Software Inc., USA) and PHOTO-Series (V7.2, PHOTON Co. Ltd., Japan), were used for geometry model building and temperature prediction. The internal volumetric heat generation term (Q , $J s^{-1} m^{-3}$) was estimated after electromagnetic field analysis based on Maxwell's equations.

【Results and Discussion】

The electric conductivity (σ), the key factor which influenced the current distribution inside food during OH, was found that increased with the temperature increasing as a linear function, explained by the less impotent opposition to the movement of the ions for higher temperature. The empirical equations were successfully obtained. And there was a logarithmic function relationship between σ and frequency. Furthermore, σ increased along with the growth of salt concentration to a certain extent.

Different components and their arrangement conditions were observed to have a significant influence on the temperature distribution during OH. For example, the completely opposite effect was found in parallel and series model. In parallel circuit, the temperature was lower in the middle where filled with mashed potato due to the easier for current to pass through the ingredient with higher σ . In contrast, the temperature was higher in mashed potato in series connection. Because the whole currents pass through each ingredient are same, while mashed potato has bigger impedance resulted in the higher temperature. Otherwise, the modeling and experiment showed a good agreement that implied a potential application for OH processing to get uniform temperature of solid composite food by electrode configurations.

Contents

Chapter 1- General Introduction	1
1.1 Background and objective	1
1.2 Literature review	2
1.2.1 Ohmic heating for food processing	2
1.2.2 Combination of ohmic with conventional heating methods.....	5
1.2.3 Ohmic heating of solid food.....	5
1.2.4 Electric conductivity	6
1.2.5 Temperature analysis during ohmic heating	7
1.2.6 Modeling of ohmic heating	8
1.2.7 Finite element method.....	9
1.2.8 Maxwell's equation	10
1.3 Structure of this dissertation.....	11
1.4 Reference.....	12
Chapter 2- Electric conductivities of materials	17
2.1 Introduction	17
2.2 Material and Methods.....	18
2.2.1 Material	18
2.2.2 Apparatus	19
2.2.3 Electric conductivity	20
2.2.4 Validation of LCR meter.....	20
2.3 Results and discussion.....	24
2.3.1 Temperature dependency of electric conductivity	24
2.3.2 Frequency dependency of electric conductivity.....	26
2.3.3 The effect of salt concentration on electric conductivity	28
2.4 Conclusion.....	29
2.5 Reference.....	29

Chapter 3- Temperature analysis during ohmic heating	31
3.1 Introduction	31
3.2 Material and Methods.....	33
3.3 Validation of ohmic heating machine	38
3.4 Check of heat generation of ohmic heating machine	40
3.5 Results and discussion.....	41
3.6 Conclusion.....	51
3.7 Reference.....	52
Chapter 4- Modeling of ohmic heating of solid food.....	54
4.1 Introduction	54
4.2 Material and Methods.....	56
4.2.1 Governing equations	56
4.2.2 The model.....	58
4.3 Validation of model.....	61
4.4 Results and discussion.....	64
4.5 Conclusion.....	77
4.6 Reference.....	78
Chapter 5- Conclusions and future work.....	81
Nomenclature	83
Acknowledgements	85

Chapter 1- General Introduction

1.1 Background and objective

The goal of thermal processing of food is to reach the designated temperature uniformly, achieve the required uniform level of sterility and minimize the structural and nutritional loss (Davies *et al.*, 1999), therefore heating is the most important unit operation among food processing. Ohmic heating is defined as a process wherein electric current is passed through materials with the primary purpose of heating them (Da-Wen Sun, 2006). It has potential to respond requirements and cope with the non-uniformity of temperature. The advantages and historical use of ohmic heating have been well documented. Compared with conventional thermal processing, ohmic heating has some advantages because heating is internally generated due to the electrical resistance within the food (Icier *et al.*, 2006) while conventional thermal processing relies on the heat transfer mechanism limited in long time consumed for conduct heat from surface to the center of food (Davies *et al.*, 1999) which may lead to the decline of quality. Ohmic heating also does a good job in energy transfer efficiency, it is observed that energy transfer efficiency of ohmic heating is close to 100% (Jun and Sastry, 2005) while microwave heating is 65% at best (Saltiel and Datta, 1999). However, food system that contains so many components with different electrical resistances is so complicated that may cause cold spot and under-processing during ohmic heating. The quality loss and safety problem will probably be incurred due to the non-uniformities in temperature distribution of food while designated temperature is crucial for the purpose of sterilization. From the safety point of view, it is important for process designer to consider the temperature distribution of non-uniform electric properties during ohmic heating. Even though ohmic heating has a limitation in uniformity related to the electric conductivity of food (M.C. Knirsch *et al.*, 2010), it has been found to be more uniform than other eletroheating techniques (Morrissey and Almonacid, 2005).

As the distortion of electric current resulted in the temperature distribution is affected by some factors such as food electric properties, physical properties, and heating conditions, calculation of changing product temperature during ohmic heating process is quite complicated and has not yet

been completely studied. It is still somewhat empirical and speculative to grasp the ohmic heating process. Therefore, it is necessary for the researchers to find the optimum heating conditions and reasonable control methods. Describing the relationship among the electric conductivity, electric field distribution and temperature is the urgent need to solve practical problems. Also extra computational work was needed to develop for understanding ohmic heating process in detail and assist in manipulating the electric conductivities of food components for uniform heating of solid composite food nowadays.

According to the reasons mentioned above, the objectives of this study were 1) to investigate the temperature distributions of four typical solid composite food systems undergoing ohmic heating combined an experimental and a computational approach considering the variable interaction effect dependent of the temperature. 2) to establish 3-D models based on finite element method (FEM) by coupling the analysis of electromagnetic field, electrical heating generation and heat transfer. All simulations were finally validated by the experiment.

1.2 Literature review

1.2.1 Ohmic heating for food processing

Ohmic heating (also called Joule heating, electrical resistance heating, direct electrical resistance heating, electroheating, or electroconductive heating) is defined as a process wherein electric currents pass through foods to heat them (Fig. 1-1). Heating is internally generated due to the electrical resistance. During ohmic heating, energy is transferred from the supplied electrical power to thermal energy. This transformation is caused by interactions between the moving particles that form the current and the atomic ions. Charged particles in an electric circuit are accelerated by the electric field but give up some of their kinetic energy each time they collide with an ion. The increase in the kinetic or vibrational energy of the ions manifests itself as heat, causing a rise in the temperature of food.

Ohmic heating is distinguished from other electrical heating methods by

(1) The presence of electrodes contacting the foods (if microwave and inductive heating electrodes are absent);

- (2) The frequency applied (unrestricted, except for the specially assigned radio or microwave frequency range);
- (3) Waveform (also unrestricted, although typically sinusoidal).

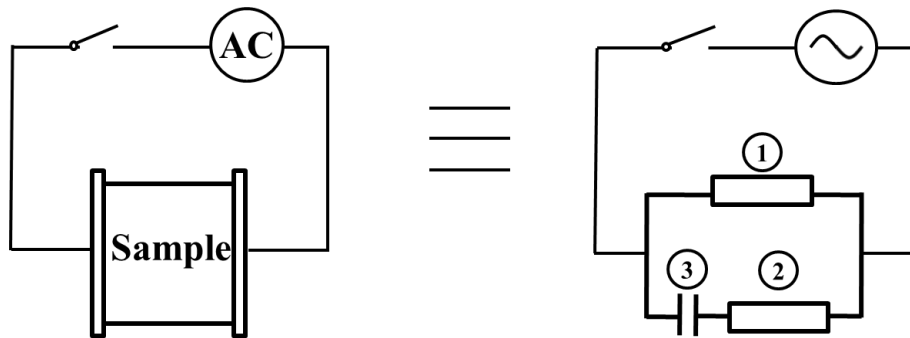


Fig. 1-1 The principle and possible equivalent circuit of ohmic heating.

- ① R_p : Resistance; ② r : Resistance caused from dielectric loss;
- ③ C : Ideal condenser

As a new commercial method for food processing, more and more attention has recently been paid to ohmic heating due to a lot of advantages it has:

- (1) uniform and rapid treatment of food with minimal heat damage and nutrient losses;
- (2) possible to heat food with low thermal conductivity rapidly;
- (3) high-temperature, short time process;
- (4) easier to control temperature precisely compared to traditional conventional heating methods;
- (5) environmentally friendly system

Being a novel energy-efficient method, ohmic heating technology origins from the end of the 19th century used for pasteurizing milk (Fowler, 1882) which has named the electropure process. At that time, ohmic heating was abandoned due to the high costs and the short of inert materials used for the electrodes (C. Amatore *et al.*, 1998). However, researches on application of ohmic

heating continued as the iron, aluminum, platinum and titanium were allowed as electrode materials by food hygiene law. The advantages claimed for this technology are uniformity of heating and improvements in quality, with minimal structural, nutritional, or organoleptic changes. The potential applications could be very wide including blanching, evaporation, dehydration, fermentation, pasteurization, and sterilization. And applications in fruits, vegetables, meat products have already been undertaken.

Recently the commercial applications of ohmic heating for the thermal processing of flowable liquid-particulate food (Markus Zell *et al.*, 2010) have been widespread. Wadad G, Khalaf and Sudhir K. Sastry (1996) reported the effect of fluid viscosity on ohmic heating rate of solid-liquid mixtures using static ohmic heating condition and continuous flow ohmic heater individually. They found out that the rate of heating increased with fluid viscosity in continuous flow ohmic heater. Filiz Icier *et al.*, (2006) pointed out the electric conductivities of apricot and peach purees are strongly dependent on temperature, ionic concentration and pulp content. They also developed a model to predict ohmic heating time of fruit purees accurately. Additional pretreatment methods such as increasing the electrolytic content in the solid, salt infusion via soaking, blanching of solids in salt solution to adjust the electric conductivities have been introduced. However, such pretreatments increase energy input and processing time. In contrast, ohmic heating of solid food materials with non-uniform electric properties is at a less advanced state of development because there is only a few of data available for heterogeneous food especially for the solid composite food, let alone explaining thermal behavior from theoretical analysis that is critical to optimize the heating uniformity of food products. Therefore, modeling of the thermal behavior of composite food products with various electric conductivities under ohmic heating has been a challenge. Halden *et al.*, (1990) pointed out that one of the key requirements for an ohmic heating system for solid products is the uniform electric conductivity within the product. Some recent papers about ohmic heating process of solid food were well documented. Markus Zell *et al.*, (2010) determined the suitability of ohmic heating to cook meat products, compared the food quality with conventionally processed samples, and noted the effect of electric conductivities on food ingredients. Much more

uniformity of microstructure and brighter in colors of meatball undergoing ohmic heating were confirmed by Wassama Engchuan *et al.*, (2014).

1.2.2 Combination of ohmic with conventional heating methods

Combined ohmic heating and conventional cooking of food has recently been patented as a new method of processing. Mechanical properties, oil and moisture content of hamburger patties were investigated by applying both plate heating and ohmic heating at the same time (Necati Özkan *et al.*, 2004). It was shown that the cooking time could be reduced and the quality of hamburger patties has insignificant differences. Markus Zell *et al.*, (2010) compared the effect of ohmic heating (HTST), LTLT which combined ohmic, hot air and conventional steam cooking on selected physical, chemical and sensory quality attributes in whole turkey meat, they found a more uniform color and lowest lipid oxidation for ohmic treatment, and the lowest cook loss for LTLT. Ohmic heating combined with cell free heating system was developed to discuss the method to minimize heat loss (M. Zell *et al.*, 2011).

1.2.3 Ohmic heating of solid food

Key requirements for an ohmic heating system for solid (i.e. meat) products include:

- (1) to make sure that sample is uniformly filled in heating cell, with a good contact between the product and the electrodes (Castro *et al.*, 2004);
- (2) to get electric conductivity within the product precisely (Halden *et al.*, 1990);
- (3) to minimize heat losses from the system (M. Zell *et al.*, 2011)

Filiz Icier and Coskan Ilicali (2005b) used tylose with different salt concentrations as a food analog for minced beef in ohmic heating. P. Pongviratchai and J.W. Park (2007) found that the starch gelatinization affected the electric conductivity as well as the color and texture qualities showed a decreasing trend with the increasing of starch concentration and decreasing of moisture content by measuring the electric conductivities of surimi-potato starch. Markus Zell *et al.*, (2009) examined the impact of the sodium chloride, phosphate and fat on electric conductivity and ohmic

heating rate and emphasized the affection of fiber orientation (perpendicular and parallel to the direction of current flow) on the electric conductivity and thermal conductivity of beef. The maximum electric conductivity of beef was proved to occur when fibers were aligned with the current flow.

1.2.4 Electric conductivity

Many factors can affect the heating rate in an ohmic heating system: electrical properties, specific heat, size, geometry and orientation in the electric field. Among these factors, electric conductivity, which is the measure of a material's ability to conduct electric current is the critical parameter of ohmic heating. Thus, knowledge of electric conductivity of food system as a whole and those of its components is essential in designing a successful ohmic heating process or for modeling. The most striking feature of electric conductivity is its dependence on temperature, as it has been shown to increase with increasing temperature. This observation is due to a variable opposition (drag force) to the movement of the ions responsible for conducting the electricity in food materials: for higher temperatures, this opposition is less important than that for lower temperature. Another major factor affecting electric conductivity is the ionic content of the food: the higher the ionic content is, the higher the value of electric conductivity will be. Moreover, electric conductivity is a function of the frequency at which it is measured.

Electric conductivity is anisotropic. Changes in the value of it reflect changes in the matrix structure, such as starch gelatinization and cell lysis. For most solid foods, electric conductivity increases sharply with temperature at around 60 °C due to the breakdown of cell wall materials, releasing ionic compounds that influenced the conductivity.

The electric conductivity is defined as:

$$\sigma = \left(\frac{1}{R}\right) \times \left(\frac{L}{A}\right) \quad (1-1)$$

Where, R is the electrical resistance of a uniform specimen of the material (Ω). L is the length of the piece of material (m). And A represents the cross-sectional area of the specimen (m^2).

Haval Y. Yacoob Aldosky *et al.*, (2011) found a cheap and convenient system with four electrodes for measuring the electric conductivity of water. M.R. Zarefard *et al.*, (2003) reported

the electric conductivity of the solid- liquid phase concerning about the particle size and concentration on heating time, especially observed the particles position which was placed in parallel, in series or in a well-mixed system. And efforts have been taken to improve the uniformity of particulate food during ohmic heating notably. Filiz Icier and Coskan Ilicali (2005a) obtained the linear temperature dependent electric conductivity relations. As well as, an accurate mathematical model was established successfully using the unsteady-state heat conduction equation by the finite difference technique. The electric conductivity of six fruits and three types of meat were found to increase linearly with temperature during ohmic heating, while fruits were less conductive than meat samples (Sanjay *et al.*, 2008). They also observed the fat distribution have a great influence on the electric conductivity of meat.

1.2.5 Temperature analysis during ohmic heating

As sterilization and food quality need to consider about the designated temperature. Damage of the food structure, color and taste occurred when overheating in contrast incomplete sterilization would be potential danger for the health of consumer when temperature doesn't reach the specific sterilization temperature. Hence the good grasp of temperature distribution and profile is the basic of controlling and optimizing the processing technology. F. Marra *et al.*, (2009) evidenced that no cold spots within the mashed potato in cylindrical batch ohmic heating cell were detected but heat loss occurred to the cell wall and electrode surface. M. Zell *et al.*, (2011), with a view to minimize heat losses during ohmic heating by designing of cell and electrode, found minimizing electrode thickness could reduce heat losses. Titaporn and Weerachet (2012) reported the temperature histories of 10 kinds of botanical beverages, concentrated juices and purees of orange and pineapple heated by a static ohmic heating system. Unless S. Salengke and S.K. Sastry (2007) investigated the ohmic heating behavior of solid-liquid mixtures at two typical sub-cases: medium-more-conductive and particle-more-conductive tending to point out the importance for considering of both static and mixed fluid situations under worst-case ohmic heating scenarios. And Suzanne A. Kulshrestha and Sudhir K. Sastry (2006) discussed the effect of end point temperature (25-70 °C) on cell membranes of food from 100 Hz to 20 kHz after ohmic treatment.

1.2.6 Modeling of ohmic heating

The main objective of ohmic heating is to reach adequate processing temperature that indicates the importance of investigation on the thermal behavior of complex system during processing, while modeling is regarded as one of the best methods because it saves time and money and can be the only way to obtain the relevant data. The models are mathematical or numerical representations which can be applied to generate the results of virtual experiments. Equations, parameters assumptions have to be taken into account in order to model the ohmic heating process. L.J. Davies *et al.*, (1999) investigated the influence of geometry on temperature differences in a solid-liquid mixture which is inhomogeneity during ohmic heating. And they used FIDAP, a commercial Computational Fluid Dynamics software package based on the finite element method and Navier-Stokes equations, to solve energy and potential field equations thus predicting the temperature. And on this basis they proposed that the accurate data on convective mixing is essential to model temperature in ohmic heating. Extra computational work based on Joule heating effect which is needed to determine the distortion of electric current resulted in the temperature distribution for both solid and liquid phases was published (W.-R. Fu and C.-C.Hsieh, 1999). S.M. Zhu *et al.*, (2010) compared the measured and predicted temperature profiles in various solid-fluid structural systems considering five theoretical models (series, parallel, two forms of Maxwell-Eucken models and effective medium theory). F. Marra *et al.*, (2009) developed a mathematical modeling to predict the heat transfer during ohmic heating of a uniform solid food incorporating appropriate electromagnetic and thermal phenomena by the use of FEMLAB, a finite element software. Xiaofei Ye *et al.*, (2004) also used FEMLAB to predict of ohmic heating then predictions were verified against temperature maps using magnetic resonance imaging (MRI). One of first three-dimensional model was established by Sastry and Palaniappan (1992). After that, Soojin Jun and Sudhir Sastry (2007) also performed a three-dimensional model for heat transfer to predict the heating patterns of tomato soup inside the pouch under ohmic heating by improving the disadvantages and optimizing of the two-dimensional model they made before which could be provide a complete thermal picture (Jun and Sastry, 2005) while the end effects could not be

considered. JaeYong Shim *et al.*, (2010) performed a modeling of thermal behavior of multiphase food products with various electric conductivities under ohmic heating using computational fluid dynamics codes (CFD). Compared with the experimental data, the maximum prediction error was 6 °C. The effects of ohmic heating on electrokinetic transport of solutes also described by the comprehensive 3D mathematical models including Poisson-Boltzmann equation, Laplace equation, modifying Navier-Stokes equation, energy equation and mass transport equation using the finite volume based on CFD technique (Gongyue Tang *et al.*, 2007).

1.2.7 Finite element method

In mathematics, the finite element method (FEM) is a numerical technique for finding approximate solutions to boundary value problems for differential equations. It uses variational methods (the calculus of variations) to minimize an error function and produce a stable solution. FEM encompasses all the methods for connecting many simple element equations over many small subdomains, named finite elements, to approximate a more complex equation over a larger domain.

FEM is useful for problems with complicated geometries, loadings, and material properties where analytical solutions cannot be obtained. The method has since been generalized for the numerical modeling of physical systems in a wide variety of engineering disciplines, r electromagnetism, heat transfer, and fluid dynamics.

In the field of ohmic heating process, the finite element model has been designed to simulate fluid with a single solid particle in a static heater using a two-dimensional model (de Alwis and Fryer, 1990). There were three types of situations for the model:

(1) *zero convection*: convective processes are less significant for example, in highly viscous and gel-forming foods.

(2) *enhanced conduction*: need to consider of the effective conductivity value which could replace the effects both convection and conduction.

(3) *well- stirred liquid*

Despite some studies in the area of mathematical model development for predicting the product temperature during ohmic heating (L.J. Davies *et al.*, 1999; W.-R. Fu and C.-C.Hsieh, 1999; J. Marafona and J.A.G. Chousal, 2006; F. Marra *et al.*, 2009), FEM was also used in other field. T.J.C. Liu (2008) analyzed the thermo-electro-structural by ohmic heating considering the cracked arrest and temperature-dependent material properties using FEM. In microwave heating, FEM was used to predict the temperature distributions in food as well (R.B. Pandit and Suresh Prasad, 2003; Noboru Sakai *et al.*, 2004; Shixiong Liu *et al.*, 2014).

1.2.8 Maxwell's equation

Electromagnetic field distribution in space and time is governed by Maxwell's equations. The differential form of Maxwell's equations can be expressed in terms of electric field and magnetic intensity (E and H), as follow:

Table 1-1. Maxwell's equations and physical interpretation

Law	Equation	Physical Interpretation
Gauss's law for B	$\nabla \cdot B = \nabla \cdot \mu H = 0$	The total magnetic flux through a closed surface is zero
Gauss's law for E	$\nabla \cdot D = \nabla \cdot \epsilon E = \rho_m$	Electric flux through a closed surface is proportional to the charged enclosed
Ampere –Maxwell law	$\nabla \times H = \frac{\partial D}{\partial t} + J = \frac{\partial \epsilon E}{\partial t} + \sigma E$	Electric current and changing electric flux produces a magnetic field
Faraday's law	$\nabla \times E = -\frac{\partial B}{\partial t} = -\frac{\partial \mu H}{\partial t}$	Changing magnetic flux produces an electric field

Where, B is magnetic induction (Wb m^{-2}), D is electric displacement (C m^{-2}), and H (A m^{-1}) and E (V m^{-1}) are the magnetic field and electric field intensity. ρ_m is the electric volume charge

density (As m^{-3}), J is current flux (A m^{-2}), ε is the complex permittivity ($\varepsilon = \varepsilon' - j\varepsilon''$ with $j^2 = -1$), and the permeability μ could be represented by $\mu_0 = 4\pi \times 10^{-7}$ (H m^{-1}), the magnetic permeability of free space. The electric conductivity σ is related to the relative dielectric loss factor of the material (ε''), $\sigma = \omega \varepsilon_0 \varepsilon''$ where ω ($\omega = 2\pi f$, f stands for the frequency of the microwave) is the angular frequency (rad s^{-1}), and $\varepsilon_0 = 8.854 \times 10^{-12}$ (F m^{-1}) is the permittivity of free space.

1.3 Structure of this dissertation

This dissertation is divided into five chapters. The main content of each part could be shown as below:

In Chapter 1, after describing the background and objectives of this research, we also reviewed the literatures about ohmic heating, electric conductivity, temperature distribution, modeling and the finite element method. And the early and latest works have given the basic theories and methods which would be applied in this study.

In Chapter 2, we investigated the electric conductivity of mashed potato and mashed potato with 1 wt % NaCl that would be used as the pseudo food materials in ohmic heating. And the electric conductivity was one of the most important properties in ohmic heating and the necessary parameter for temperature predicting. The electric conductivity of materials were measured by LCR meter using water bath from 10 °C to 85 °C, at 5 °C intervals. The influences of frequency and temperature were examined and discussed.

In Chapter 3, temperature distributions of four different filling patterns designed with respect to the parallel, series and surrounding connections when connected with electrodes after ohmic heating were investigated. And during heating, an ohmic heating machine was applied for supplying the alternating current (50 V, 20 kHz) and four thermocouples at different typical positions were used to record the temperature profiles. After that the thermal pictures of the cross-section were captured by an infrared thermal camera which would be used to verify the estimations of model explained in chapter 4.

In Chapter 4, a three-dimensional computer model based on finite element method was developed to predict time-dependent temperature distributions of food sample during ohmic heating with considering the electromagnetic field analysis and heat transfer whereas the node

coordinate and dielectric properties of sample were updated with time steps, and the heat generations were renewed according to these parameters. We settled the size of the real cell in the geometric model using a software named FEMAP, and calculated the electric field based on Maxwell's equation temperature using PHOTON. In simulation, mesh size, interface assignment in geometric model, iterations setting, time steps and electric field strength that would directly or indirectly affect the analysis of electromagnetic field and heat transfer were discussed. Methods for approximating simulating the temperature proposed and discussed in view of sample's shape and electric properties to achieve the minimum computational time and were experimentally validated by comparing with temperature distributions captured by an infrared thermal camera.

In Chapter 5, we summarized the general outline and concluded the main results from this research. Also we sum up the prospect of future applications of modeling of temperature distribution in solid food during ohmic heating by using finite element methods and pointed out the difficulty where we need to pay more attention on.

1.4 Reference

De Alwis A.A.P., & Fryer P.J. (1990). The use of network theory in the finite-element analysis of coupled thermo-electric fields. *Communications of Applied Numerical Methods*, 6, 61-66.

C. Amatore., M. Berthou., S. Hébert. (1998). Fundamental principles of electrochemical ohmic heating of solution. *Journal of Electroanalytical Chemistry*, 457, 191-203.

Craig Saltiel., & Ashim K. Datta. (1999). Heat and mass transfer in microwave processing. *Advances in Heat Transfer*, 33 (1), 1-94.

Filiz Icier., & Coskan Ilicali. (2005a). Temperature dependent electrical conductivities of fruit purees during ohmic heating. *Food Research International*, 38, 1135-1142.

Filiz Icier., & Coskan Ilicali. (2005b). The use of tylose as a food analog in ohmic heating studies. *Journal of Food Engineering*, 69, 67-77.

- Filiz Icier., Hasan Yildiz., Taner Baysal. (2006). Peroxidase inactivation and colour changes during ohmic blanching of pea puree. *Journal of Food Engineering*, 74, 424-429.
- F. Marra., M. Zell., J.G. Lyng., D.J Morgan., D.A. Cronin. (2009). Analysis of heat transfer during ohmic processing of a solid food. *Journal of Food Engineering*, 91, 56-63.
- Fowler A. (1882). Apparatus for preserving meats. *U.S. patent*, 267, 685.
- Gongyue Tang., Deguang Yan., Chun Yang., Haiqing Gong., Cheekiong Chai., Yeecheong Lam. (2007). Joule heating and its effects on electrokinetic transport of solutes in rectangular microchannels. *Sensors and Actuators A*, 139, 221-232.
- Halden K., De Alwis A.A.P., Fryer P.J. (1990). Changes in the electrical conductivity of foods during ohmic heating. *International Journal of Food Science and Technology*, 25 (1), 9-25.
- Haval Y. Yacoob Aldosky., & Suzan M. H. Shamdeen. (2011). A new system for measuring electrical conductivity of water as a function of admittance. *Journal of Electrical Bioimpedance*, 2, 86-92.
- I. Castro., J.A. Teixeira., S. Salengke., S.K. Sastry., A.A. Vicente. (2004). Ohmic heating of strawberry products: electrical conductivity measurements and ascorbic acid degradation kinetics. *Innovative Food Science and Emerging Technologies*, 5 (1), 27-36.
- JaeYong Shim., Seung Hyun Lee., Soojin Jun. (2010). Modeling of ohmic heating patterns of multiphase food products using computational fluid dynamics codes. *Journal of Food Engineering*, 99, 136-141.
- J. Marafona., & J.A.G. Chousal. (2006). A finite element model of EDM based on the Joule effect. *International Journal of Machine Tools & Manufacture*, 46, 595-602.
- Jun S., & Sastry S (2005). Modeling and optimizing of pulsed ohmic heating of foods inside the flexible package. *Journal of Food Engineering*, 28 (4), 417-436.
- L.J. Davies., M.R. Kemp., P.J. Fryer. (1999). The geometry of shadows: effects of inhomogeneities in electrical field processing. *Journal of Food Engineering*, 40, 245-258.

- M.C. Knirsch., C.A. dos Santos.,A.A.M. de Oliveira Soares Vicente., T.C.V. Penna. (2010). Ohmic heating- a review. *Trends in Food Science & Technology*, 21, 436-441.
- Markus Zell., James G. Lyng., Denis A. Cronin ., Desmond J. Morgan. (2009). Ohmic heating of meats: Electrical conductivities of whole meats and processed meat ingredients. *Meat Science*, 83, 563-570.
- Markus Zell., James G. Lyng., Denis A. Cronin ., Desmond J. Morgan. (2010). Ohmic heating of whole turkey meat- effect of rapid ohmic heating on selected product parameters. *Food Chemistry*, 120, 724-729.
- Michael T. Morrissey., & Sergio Almonacid. (2010). Rethinking technology transfer. *Journal of Food Engineering*, 67, 135-145.
- M. R. Zareifard., H.S. Ramaswamy., M. Trigui., M. Marcotte. (2003). Ohmic heating behaviour and electrical conductivity of two-phase food systems. *Innovative Food Science and Emerging Technologies*, 4, 45-55.
- M. Zell., J.G. Lyng., D.J Morgan., D.A. Cronin. (2011). Minimising heat losses during batch ohmic heating of solid food. *Food and Bioproducts Processing*, 89, 128-134.
- Necati Özkan., Ian Ho., Mohammed Farid. (2004). Combined ohmic and plate heating of hamburger patties:quality of cooked patties. *Journal of Food Engineering*, 63, 141-145.
- P. Pongviratchai., & J.W. Park. (2007). Electrical conductivity and physical properties of surimi-potato starch under ohmic heating. *Journal of Food Science*, 72 (9), 503-507.
- R.B. Pandit., &Suresh Prasad. (2003). Finite element analysis of microwave heating of potato- transient temperature profiles. *Journal of Food Engineering*, 60, 193-202.
- Sanjay Sarang., Sudhir K. Lynn Knipe. (2008). Electrical conductivity of fruits and meats during ohmic heating. *Journal of Food Engineering*, 87, 351-356.
- S.K. Sastry., & S. Palaniappan. (1992). Mathematical modelling and experimental studies on ohmic heating of liquid-particle mixtures in a static heater. *Journal of Food Process Engineering*, 15 (4), 241-261.

- Shixiong Liu., Yoshiko Ogiwara., Mika Fukuoka., Noboru Sakai. (2014). Investigation and modeling of temperature changes in food heated in a flatbed microwave oven. *Journal of Food Engineering*, 131, 142-153.
- S.M. Zhu., M.R. Zareifard., C.R. Chen., M. Marcotte.,S. Grabowski. (2010). Electrical conductivity of particle-mixtures in ohmic heating: Measurement and simulation. *Food Research International*, 43, 1666-1672.
- Soojin Jun., & Sudhir Sastry. (2007). Reusable pouch development for long term space mission: a 3D ohmic model for verification of sterilization efficacy. *Journal of Food Engineering*, 80, 1199-1205.
- S. Salengke., & S.K. Sastry. (2007). Experimental investigation of ohmic heating of solid-liquid mixtures under worst-case heating scenarios. *Journal of Food Engineering*, 80, 324-336.
- Suzanne A. Kulshrestha., & Sudhir K. Sastry. (2006). Low-frequency dielectric changes in cellular food material from ohmic heating: Effect of end point temperature. *Innovative Food Science and Emerging Technologies*, 7, 257-262.
- Titaporn Tumpanuvatr., & Weerachet Jittanit. (2012). The temperature prediction of some botanical beverages, concentrated juices and purees of orange and pineapple during ohmic heating. *Journal of Food Engineering*, 113, 226-233.
- T.J.C. Liu. (2008). Thermo-electro-structural coupled analyses of crack arrest by Joule heating. *Theoretical and Applied Fracture Mechanics*, 49, 171-184.
- Wadad G. Khalaf., & Sudhir K. Sastry. (1996). Effect of viscosity on the ohmic heating rate of solid-liquid mixtures. *Journal of Food Engineering*, 27, 145-158.
- Wassama Engchuan., Weerachet Jittanit., Wunwiboon Garnjanagoonchorn. (2014). The ohmic heating of meat ball: Modeling and quality determination. *Innovative Food Science and Emerging Technologies*, 23, 121-130.

W.-R Fu., & C.-C Hsieh. (1999). Simulation and verification of two-dimensional ohmic heating in static system. *Journal of Food Science*, 64 (6), 946-949.

Xiaofei Ye., Roger Ruan., Paul Chen., Christopher Doona. (2004). Simulation and verification of ohmic heating in static heater using MRI temperature mapping. *Lebensm.-Wiss. u.-Technol*, 37, 49-58.

Chapter 2- Electric conductivities of materials

2.1 Introduction

As the key parameter of ohmic heating, the critical electric conductivity of food is from 0.01 S m^{-1} to 10 S m^{-1} where ohmic heating is applicable (M.C. Knirsch *et al.*, 2010). Beyond of this range, the very large voltages or very large amperage values were difficult to apply for ohmic heating to generate the amount of heat required raising temperature substantially by the Joule effect.

Many published works proved that the food products with high salt or acid contents would have high electric conductivity and ohmic heating rate; in contrast, an increase in fat content with poor conductivity acting as the barrier for the passage of electrical current results in the low electric conductivity (Titaporn and Weerachet, 2012). Increasing the electrolytic content within foods to increase electric conductivity may be accomplished by salt infusion via soaking or blanching of solids in salt solution. This may be used as a pretreatment for achieving the ideal ohmic heating situation to get the uniform temperature distribution with the same heating rate of each ingredients, if the composition and other properties of the food are not greatly affected.

Anisotropic of electric conductivity was also vary pronouncedly in the literature. Changes in the value of it reflect changes in the matrix structure, such as starch gelatinization and cell lysis. For example, the electrical conductance of potato can be 0.06 S m^{-1} (De Alwis, Halden and Fryer, 1989), 0.037 S m^{-1} (Kim *et al.*, 1996), or 0.32 S m^{-1} (Palaniappan and Sastry, 1991).

Furthermore, the most striking feature of electric conductivity is its dependence on temperature and frequency, as it has been shown to increase with increasing temperature pointed out by Filiz Icier and Coskan Ilicali (2005) and Sanjay *et al.*, (2008)

In non-homogeneous materials, such as liquid-solid mixtures, the electric conductivity of the particles and its relation to the fluid conductivity is pointed as a critical parameter (M.R. Zarefard *et al.*, 2003). Proper electric conductance management is essential to ohmic heating

of foods.

To model the system successfully, accurate electric conductivities of two ingredients which were the important parameters used for temperature analysis and modeling were required. The aim of this chapter was to measure the electric conductivity of two materials used as solid food analog the pseudo food which are mashed potato and mashed potato with 1wt % sodium chloride and to clarify the effect of temperature, frequency and salt concentration on electrical electivity, preparing the data base for temperature analysis and model during ohmic heating.

2.2 Material and Methods

2.2.1 Material

Reconstituted potato preparation Reconstituted dried potatoes were chosen as the pseudo solid food in this study because of their highly homogenous nature (M. Zell *et al.*, 2011) by neglecting the starch gelatinization, destabilization of cellular membranes, cell electroporation, tissue shrinkage, which are pointed to be the main responsible effect for the change of the system's electric conductivity (M.C. Knirsch *et al.*, 2010). Two materials used as solid food analog the pseudo food composed of two ingredients to allow differing electrical properties which are mashed potato (material A) and mashed potato with 1wt % sodium chloride (material B) were prepared. For the preparation of mashed potato, the ratio of instant mashed potato flakes (Mashed Potato Tokuyo1201, Marukyu Co. Ltd., Japan; crude protein content was above 4.8 %, crude fat content was below 0.9 %, crude ash content was below 2.7 % and carbohydrate content was about 95.2 %) to distilled water was 80 to 20. And for mashed potato with 1 wt % sodium chloride, instant mashed potato flakes, distilled water and sodium chloride in the ratio 80: 20: 1. The thermal properties and composition of two ingredients were show in Table 2-1. Subsequently samples were stirred (10 min) into the homogeneous mixture respectively. The samples were sealed with cling film to prevent evaporative moisture loss. The formulations were then kept at 25 °C about 3 hours until the water was fully absorbed and the moisture migration was finished. After that, material A and B were filled into rectangular parallelepiped plastic cuvettes (10 ×10 ×43 mm) using an injector with a long rubber hose.

Table 2-1. Thermal properties and composition of two materials

Material	Water content	Salted addition (NaCl)	Density (g cm ⁻³)	Specific heat (J kg ⁻¹ °C ⁻¹)	Thermal conductivity (W m ⁻¹ °C ⁻¹)	Electric conductivity (S m ⁻¹)
A	80%	0%	1.0	4189.9	0.6049	0.0063T+0.1712
B	80%	1%	1.0	4184.9	0.6049	0.0227T+0.9459

2.2.2 Apparatus

Experiments were conducted in a water bath cell (O), shown schematically in Fig. 2-1. One of the rectangular parallelepiped plastic cuvettes was used to hold sample between two titanium electrodes (9 × 57 mm), thickness was (0.5 mm). The gap between the electrodes was 10 mm. Another cuvette with the same material was used to control the center temperature of samples using a K-type thermocouple ($\phi = 0.5$ mm) inserted to the geometric center of the sample preventing the influence of existence of thermocouple on the impedance. The temperature of the samples was allowed to equilibrate to an initial temperature of 20 ± 0.2 °C in a water bath maintained at that temperature before the heating was started. The samples were sealed with cling film to prevent evaporative moisture loss and moisture migration between vapor from water bath and sample.

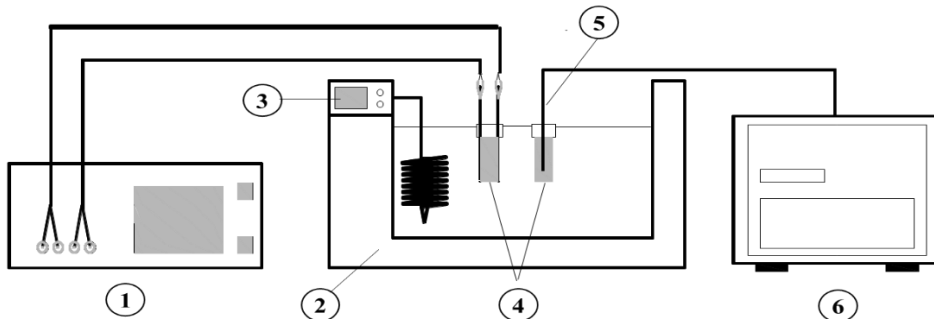


Fig. 2-1 Apparatus for electric conductivity measurement.

- ① LCR meter; ② water bath; ③ heating equipment;
④ materials; ⑤ thermocouple; ⑥ datalogger

The resistance of the two materials was measured 5 °C intervals from 20 to 80 °C respectively by LCR meter as shown in Fig. 2-2 (HiTESTER3532-50, HIOKI Co. Ltd., Japan) at frequencies ranging from 42 Hz to 5 MHz and measure the instantaneous impedance, resistance and reactance just spending 72 ms.



Fig. 2-2 LCR meter (HiTESTER3532-50, HIOKI Co. Ltd., Japan)

A personal computer, a datalogger (Thermodac 5001A, Eto Denki Co., Tokyo, Japan), software (Thermodac-E/Ef 2.6, Eto Denki Co.) were used to collect the temperature data and electrical properties data. All experimental runs were carried out in triplicate.

2.2.3 Electric conductivity

The electric conductivity (σ , S m⁻¹), was determined from the geometry of the cell and the resistance using Eq. (2-1).

$$\sigma = \left(\frac{1}{R}\right) \times \left(\frac{L}{A}\right) \quad (2-1)$$

Where, R is the resistance of the material (Ω). L is the gap between two electrodes (m). And A represents the cross-sectional area of the material in the heating cell (m²).

2.2.4 Validation of LCR meter

The potassium chloride standard solution (the concentration of KCl solution: 20, 50, 100, 200, 500 mM) was used to investigate the frequency dependency of electric conductivity and

verify the accuracy of LCR meter by comparing with the data reported. The 1 L KCl solution was poured into the static ohmic heating cell (100 ×100 × 100 mm) with two titanium plate electrodes (thickness is 2 mm) inserted the parallel internal wall of cell. Then the impedance measured by LCR meter at frequency of 50, 60, 100, 150, 300, 500, 1000, 2500, 5000, 7500, 10 k, 20 kHz at certain temperature and calculated the electric conductivity by Eq. (2-1).

From Fig. 2-3, we found that when the concentration of KCl solution was below 200 mM, the electric conductivity at 20 kHz was almost same with the data from reference which was under the direct current condition at 25 °C. While when the concentration of KCl solution was 500 mM, there was just about 0.7 S m⁻¹ difference between them that considered LCR meter had a high reliability at 20 kHz.

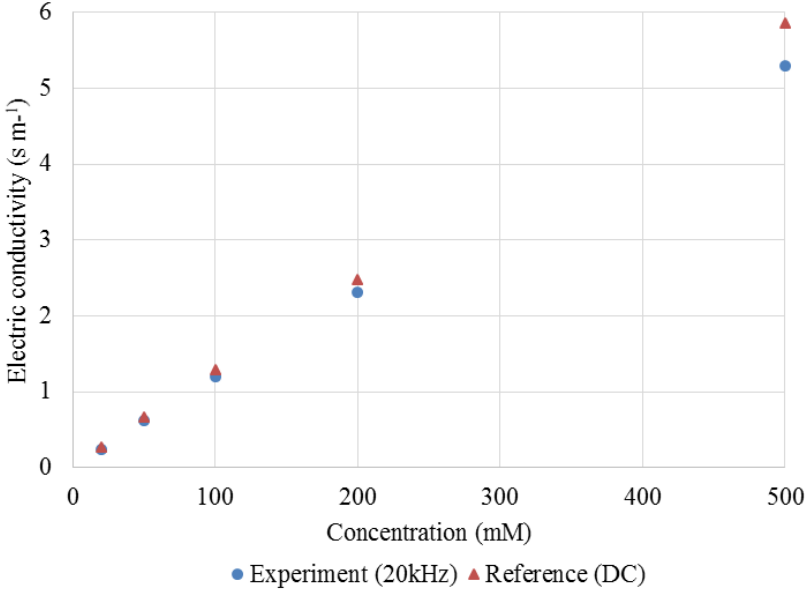


Fig. 2-3 Electric conductivity of KCl solution at different concentration at 20 kHz (25 °C).

Fig. 2-4 showed that at room temperature, the electric conductivity of 100 mM was increasing with the frequency rising. And at low frequency the values of electric conductivity from Z , R_s , R_p had a great difference. However, when the frequency was above 500 Hz, the three values tended to be the same. Also when the frequency was larger than 5000 Hz, the electric conductivity showed the constant value 1.29 S m⁻¹ the same with the value of reference at the

direct current situation. This result was consistent in agreement with Fig. 2-5 where we used mashed potato as the samples.

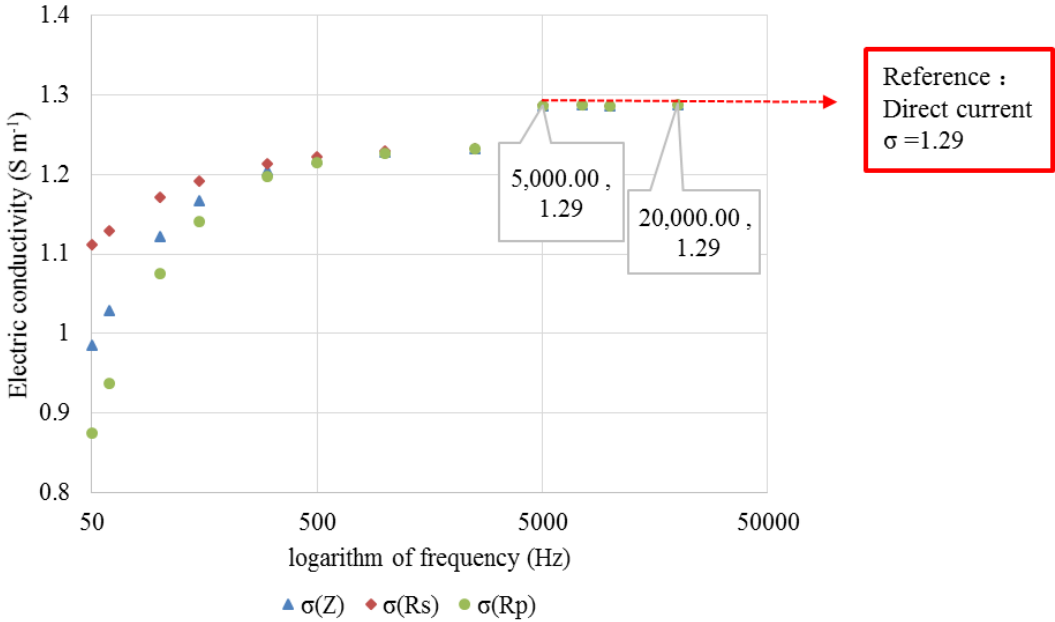


Fig. 2-4 Electric conductivity of 100 mM KCl solution at frequency of 50, 60, 100, 150, 300, 500, 1000, 2500, 5000, 7500, 10k, 20k Hz (25 °C).

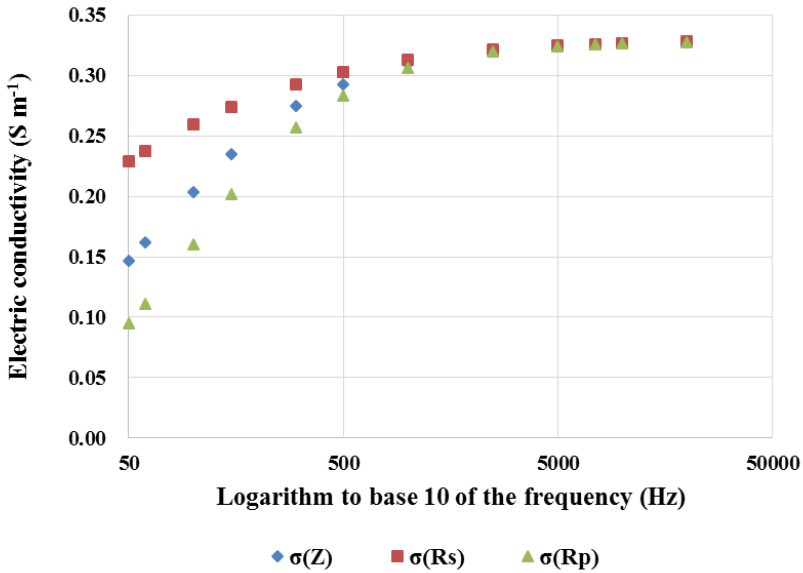


Fig. 2-5 Electric conductivity of mashed potato at frequency of 50, 60, 100, 150, 300, 500, 1000, 2500, 5000, 7500, 10k, 20k Hz (25 °C).

When Z , R_s , R_p was mentioned, the way of electrical circuit connected had to be talked about. The two simplest circuits called series and parallel occur very frequently. Similarly, the resistances also have the series resistance and parallel resistance. For alternating current circuit, different frequency bands would bring different effects of capacitance in resistances. Thus, when thinking about the resistance value of the sample, we should take three kinds of resistances into consideration: Z , the impedance; R_s , the resistance component of the series circuit; and R_p , the resistance component of the parallel circuit. What we want to know was, in ohmic heating, would capacitance or dielectric have any effects on the resistance value. When we put the food in one of the circuits, we could represent these three kinds of resistances just like the Fig. 2-6. We could consider Z as an effective resistance, and R_p as the resistance value of parallel circuit with a resistance component in it, and R_s as the resistance value of series circuit with a resistance component in it. When we set up the circuits, the calorific value of these circuits calculated from the voltage and the electric current would be different from each other. In this study, we calculated the electric conductivity using Z simply owing to the same value of Z , R_s , R_p at 20 kHz.

The impedance, Z , is composed of real and imaginary parts:

$$Z = R + jX \tag{2-2}$$

Where, R is the resistance (Ω), X is the reactance (Ω)

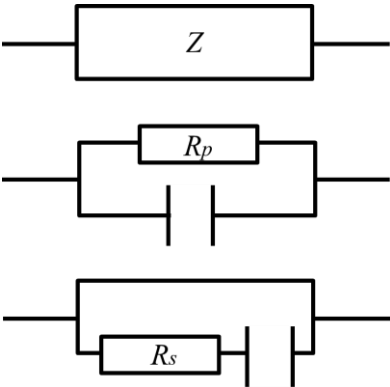


Fig. 2-6 Three kinds of resistances in alternating current circuit (Z , the impedance; R_s , the resistance component of the series circuit; and R_p , the resistance component of the parallel circuit).

2.3 Results and discussion

2.3.1 Temperature dependency of electric conductivity

The measured electric conductivity value of mashed potato (material A) and mashed potato with 1wt % sodium chloride (material B) are plotted at 50 Hz, 60 Hz and 20 kHz in Fig. 3-7 and Fig. 3-8, respectively. Electric conductivity of sample was characterized as a function of temperature. The value of electric conductivity rose with the temperature increasing as a linear function for every frequency with a relative high coefficient for electric conductivity measured from 20 to 80 °C for material A and B. This phenomenon occurred because that the opposition to the movement of the ions for higher temperatures was less important than for lower temperature. And regression analysis resulted in the following empirical equation:

$$\text{A: } \sigma = 0.0063T + 0.1712$$

$$\text{B: } \sigma = 0.0227T + 0.9459$$

Where T is the temperature (°C).

From Fig. 2-7 and Fig. 2-8, we could clearly conclude that at initial temperature the electric conductivity of mashed potato at 20 kHz was about two times larger than that at 50 Hz as the value of 0.291 and 0.149 S m⁻¹, respectively. With the temperature rising, the difference was much bigger for the slope of the curve at 20 kHz. It was about three times larger than that at 50 and 60 Hz apparently. It means that the increasing rate of electric conductivity following temperature at high frequency was much more rapid than that of low frequency, thus the temperature dependency of conductivity showed increasing trending with the rising of frequency. In other words, the temperature dependency of conductivity behaved more obvious at high frequency compared to the low frequency 50 and 60 Hz which were usually used as the domestic frequency. Besides, the difference of electric conductivity at 50 and 60 Hz was not significant. Likewise, the same trend showed in salted mashed potato but more serious.

Around 60 °C, starch began to gelatinization in general conditions which produced important influence on technological art, quality and structure of starch food while the electric conductivity of material A and B haven't shown sharp change in value, because reconstituted potato was under hot-air drying and rehydration before using as the samples.

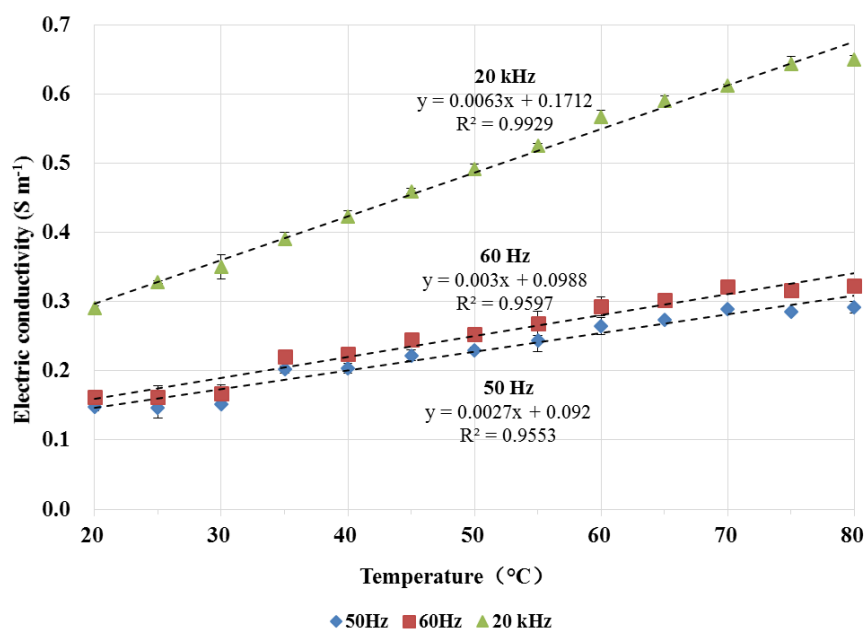


Fig. 2-7 Electric conductivity of mashed potato as a function of temperature at frequency of 50, 60 and 20k Hz.

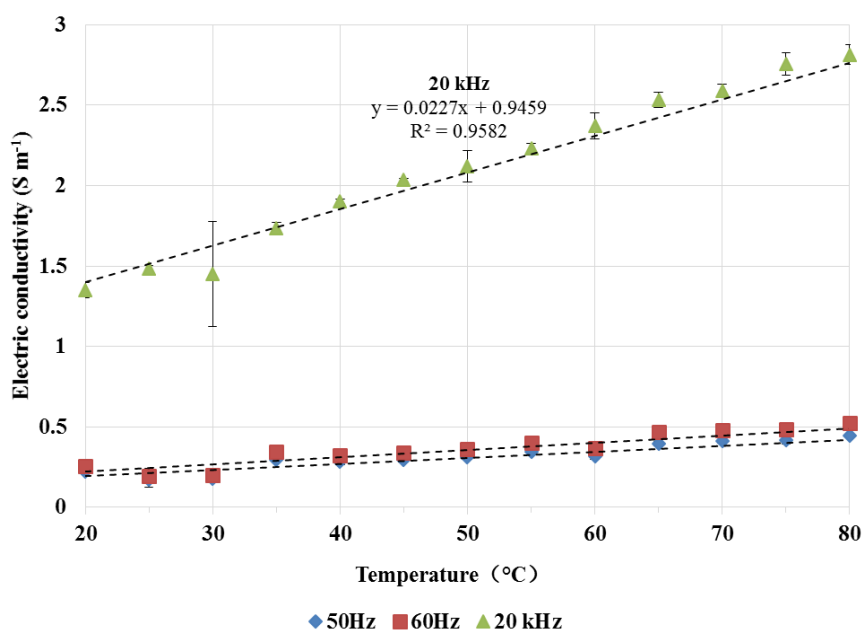


Fig. 2-8 Electric conductivity of mashed potato with 1 wt % sodium chloride as a function of temperature at frequency of 50, 60 and 20k Hz.

2.3.2 Frequency dependency of electric conductivity

Fig. 2-9 and 2-10 demonstrated the electric conductivity changes with the various frequency. The plotting results indicated that there were logarithmic function relationships between them. As the frequency increased, the electric conductivity of both component materials showed the same trend that below the certain frequency the electric conductivity was rising with the increasing of frequency at all measured temperature, above the certain frequency, the increasing rate became smaller until the values were stable. Nevertheless, the certain frequency was 2500 Hz for mashed potato and 7500 Hz for salted mashed potato. And below the certain temperature, the increasing rate of electric conductivity in salted mashed potato was much more rapid than that of mashed potato. That was to say, the salted mashed potato was more sensitive associated with frequency than mashed potato.

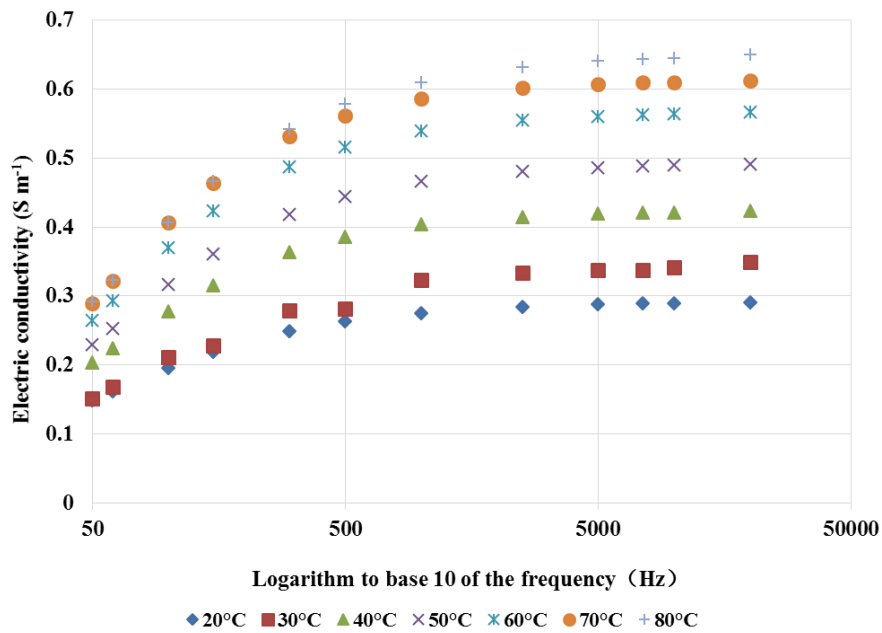


Fig. 2-9 Electric conductivity of mashed potato as a function of frequency from 20 to 80 °C.

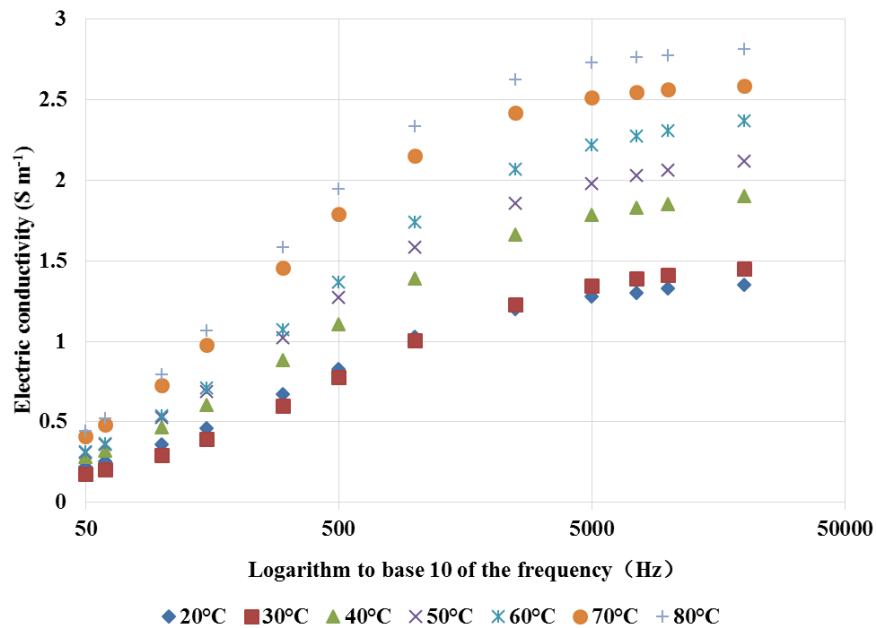


Fig. 2-10 Electric conductivity of mashed potato with 1 wt % sodium chloride as a function of frequency from 20 to 80 °C.

However, at low frequencies the calculation of electric conductivity was subject to errors due to electrode polarization. (Suzanne A. Kulshrestha and Sudhir K. Sastry, 2006) estimated the effect of electrode capacitance by comparing raw potato samples to isoconductive KCl solution. They found that at 100 Hz the conductivity of potato cylinders heated by water bath increased sharply above 50 °C while that of ohmically heated samples increased more gradually and became significantly higher at 40 °C endpoint temperature. However, at 20 kHz, the electric conductivity was almost the same at certain temperature. They also pointed out that above 5 kHz, the cell membrane lose their selectivity, the ionic double layers on membrane surface, caused by negative charge accumulation within the cell, are not available to provide a capacitive reactance within the time scales. In other words, at high frequency the membrane permeability was relatively less affected on the electric conductivity. In our study, the influence of membrane permeability which results in gradual change in electric conductivity could be ignored because of irreversible inactivation in cell of reconstituted potato after hot-air drying and rehydration.

2.3.3 The effect of salt concentration on electric conductivity

Fig. 2-11 evidenced the electric conductivity results from material A and B considering frequency at 50 Hz and 20 kHz. The electric conductivity of 1 wt % salt contained mashed potato was higher than that of mashed potato at both frequency while this trend appeared up to about five times at 20 kHz measured at the same temperature. It means electric conductivity increased along with the growth of salt concentration for material A and B to a certain extent. And they showed the same trend with KCl solution. Also it was obvious that electric conductivity increasing rate of salted mashed potato with temperature was much sharper than that of mashed potato of both frequency. The salts are normally dissociated to be ions and act as the electrical current carriers during ohmic heating. In addition, within the same material, the difference of electric conductivity value was not remarkable at 50 Hz when compared to that measured at 20 kHz.

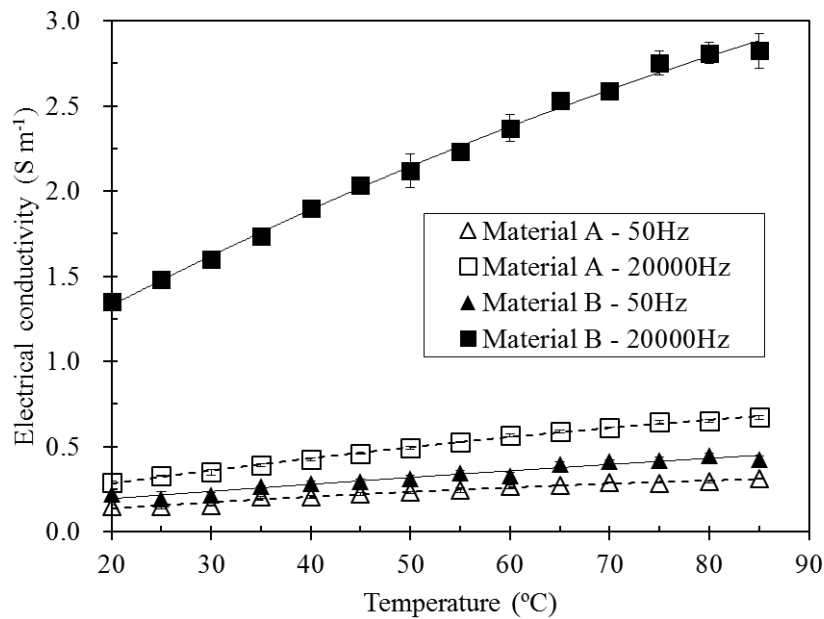


Fig. 2-11 Electric conductivity of mashed potato (material A) and mashed potato with 1 wt % sodium chloride (material B) at 50 Hz and 20 kHz from 20 to 85 °C.

2.4 Conclusion

The electrical conductivities of each material used in ohmic heating were established respectively that to lay a good foundation on data base for modeling the temperature distribution during ohmic heating. We also clarified the effect of temperature, frequency, salted concentration on electric conductivity. The relationships between them were obtained as follow:

1. The electric conductivity increased with the temperature increasing as a linear function from 20 to 80 °C, explained by the less impotent opposition to the movement of the ions for higher temperature. And the empirical equations were successfully obtained.
2. There were a logarithmic function relationship between electric conductivity and frequency. Below the certain frequency, the electric conductivity of both component materials was rising with the frequency increasing, above that the increasing rate became slow until the values were stable.
3. Electric conductivity increased along with the growth of salt concentration for material A and B to a certain extent.

In addition, aluminum electrode was found to be corroded in sodium chloride solution at 50 Hz of literature. And it was not possible to calculate the influence of the electrode on electric conductivity without enough accuracy for a rigorous correction of the data. Therefore, we finally determined to use 20 kHz as the frequency of ohmic heating in order to eliminate the influence.

2.5 Reference

De Alwis A. A. P., Halden K., Fryer P. J. (1989). Shape and conductivity effects in the ohmic heating of foods, *Chemical Engineering Research and Design*, 67, 159-168.

Filiz Icier., & Coskan Ilicali. (2005). Temperature dependent electrical conductivities of fruit purees during ohmic heating. *Food Research International*, 38, 1135-1142.

Kim H. J., Choi Y. M., Yang T. C. S., Taub I. A., Tempest P., Skudder P. (1996). Validation of OH for quality enhancement of food products. *Food Technology*, 50, 253-261.

- M.C. Knirsch., C.A. dos Santos.,A.A.M. de Oliveira Soares Vicente., T.C.V. Penna. (2010). Ohmic heating- a review. *Trends in Food Science & Technology*, 21, 436-441.
- M.R. Zareifard., H.S. Ramaswamy., M. Trigui ., M. Msrcotte. (2003). Ohmic heating behaviour and electrical conductivity of two-phase food systems. *Innovative Food Science and Emerging Technologies*, 4, 45-55.
- M. Zell., J.G. Lyng., D.J Morgan., D.A. Cronin. (2011). Minimising heat losses during batch ohmic heating of solid food. *Food and Bioproducts Processing*, 89, 128-134.
- Palaniappan S., & Sastry S. K. (1991). Electrical conductivities of selected solid foods during ohmic heating. *Journal of Food Process Engineering*, 14, 221-236.
- Sanjay Sarang., Sudhir K. Lynn Knipe. (2008). Electrical conductivity of fruits and meats during ohmic heating. *Journal of Food Engineering*, 87, 351-356.
- Suzanne A. Kulshrestha., & Sudhir K. Sastry. (2006). Low-frequency dielectric changes in cellular food material from ohmic heating: Effect of end point temperature. *nnovative Food Science and Emerging Technologies*, 7, 257-262.
- Titaporn Tumpanuvat., Weerachet Jittanit. (2012). The temperature prediction of some botanical beverages, concertrated juices and purees of orange and pineapple during ohmic heaing. *Journal of Food Engineering*, 113, 226-233.

Chapter 3- Temperature analysis during ohmic heating

3.1 Introduction

The internal heat generation induced by ohmic heating eliminates the problems associated with heat conduction in food material, preventing the overcooking of conventional thermal food processing. Moreover, as the heating process is generally faster than that with heat exchangers, the killing of microbial cultures is obtained with a less pronounced degradation of most food components. Therefore, ohmic heating is an alternative fast heating method which could improve the safety and quality of food products. In spite of the benefit ohmic heating has, it also has some limitations because the heat generation during ohmic heating is directly related to the electric conductivity of food. While various reactions must be considered to occur in a food matrix that includes in its composition several components with different electrical, heat, mass, and momentum transfer properties. Thus, the foods with lower electric conductivities will be heated slower than those with higher electric conductivities if the same electrical field strength is applied. In other words, to obtain the same heating rate more intense electrical field strength is needed for the lower conductive food. The phenomena that cause uninform heating must be understood to minimize this shortcoming, while modeling of ohmic heating tends to be one of the best way for this type of investigation.

In previous work, the most successful commercial applications of food in ohmic heating process were in liquid and particle-fluid mixtures (JaeYong Shim *et al.*, 2010; S.M. Zhu *et al.*, 2010; S. Salengke and S.K. Sastry, 2007; Xiaofei Ye *et al.*, 2004; Y. Benabderrahmane and J.-P. Pain, 2000; L.J. Davies *et al.*, 1999; W.-R Fu *et al.*, 1999; Wadad G. Khalaf and Sudhir K. Sastry, 1996; S.K. Sastry and S. Palaniappan, 1992). In contrast, solid food materials are under less advanced due to the difficulty in providing good contact between the electrodes and the food surface. Recently, several studies of the thermophysical properties of meat products have been well documented (Wassama Engchuan *et al.*, 2014; Markus Zell *et al.*, 2009, 2010; N. Shirsat *et al.*, 2004) that revealed the potential to cook meat products using ohmic heating.

Several applications have been proposed and developed for ohmic heating in relation to

microbial control to replace the heating methods for food pasteurization, sterilization and food processing such as blanching, evaporation, dehydration, fermentation and extraction. And several units are already working at the industrial scale. The characterization, modeling, and control of all the phenomena associated with the application of ohmic heating in food processing will lead to the achievement of the main goal: to have an effective control on temperature profile of food materials during heating foods (Xiaofei Ye *et al.*, 2004).

Since the main critical factor in thermal processes is the thermal history and location of the “cold spot”, locating cold zones during ohmic heating requires special consideration as the current knowledge of ohmic heating technology (L.J. Davies *et al.*, 1999). Obviously, each individual component and their interactions will play a decisive role in the efficiency of the ohmic heating process (S.M. Zhu *et al.*, 2010). Such a role may be played on the thermal killing of the microbial population or on the modification of the functional, nutritional, and organoleptic properties of foods. This reasoning clearly points out the complexity associated with thermal processing of foods especially in ohmic heating.

Consequently, to develop models that will allow for a more precise mapping of temperatures on foods submitted to ohmic heating. And to be the foundation for characterizing the effect of ohmic heating on nutritive, organoleptic, and functional properties of solid foods in the future, this work should be initiated by studying the effects on each individual food components, extending to whole simplified pseudo food (Filiz Icier and Coskan Ilicali., 2005), and implementing a model to predict temperature distribution under four typical solid food systems filled by mashed potato with different salt concentration so that an adequate control of the rate of heating and an suitable design of the ohmic heaters by adjusting the pattern of ohmic heating system adapted to specific food processes for minimizing the thermal degradation effects on desirable products can be achieved. The purpose of this chapter was to estimate the temperature distribution of four typical filling patterns: the parallel (parallel to electric current) and series model (perpendicular to electric current) and two typical surrounding-cases: pure-inside-salt model and salt-inside-pure model and provide experimental verification for model trends. The current study is principally intended to gain a deeper understanding of electric field distribution,

and whether model predictions are consistent with specific experimental observations.

3.2 Material and Methods

Mashed potato (material A) and mashed potato with 1 wt % sodium chloride (material B) were prepared using reconstituted potato as mentioned in chapter 2 and then filled into the static ohmic heating cell after the water was fully absorbed and the moisture migration was finished. Fig. 3-1 represents the schematic of the static ohmic heating cell. The heater consisted of a polypropylene container (100 × 80 × 50 mm measured in inner, thickness of the container is 5 mm) with two titanium plate electrodes (80 × 65 mm, thickness is 1 mm) at each end. And the cell was cut into two parts equally in height (each of them is 25 mm in inner). From a macroscopical standpoint of theoretical model, four filling patterns (as shown in Fig. 3-2) designed for basic structures of two-ingredient typical food system were used to measure and model the temperature distributions during ohmic heating. The distance between the two electrodes was set as 100 mm. Through the electrodes, the 20 kHz alternating current was supplied at 50 V via a voltage regulator (HJU3000-HF-30, HANO Co. Ltd., Japan), this gave an electrical field strength of 707.1068 V m⁻¹ and the container was besieged by foam-plastic to insulate heat transfer between sample and environment. Four pieces of K-type thermocouple probes ($\phi = 0.5$ mm), coated with Teflon to protect interference with the electrical field were inserted from the top through the center of a plastic tubing ($\phi = 2.2$ mm) in the center of height to monitor the temperatures in four different locations during ohmic heating. Care was exercised to ensure that the thermocouples measuring the particle center temperature was inserted at the same depth and distance from end faces for every run. Thermocouple signals were transmitted to the data acquisition unit (Thermodac 5001A, Eto Denki Co., Tokyo, Japan) collected with a software (Thermodac-E/Ef 2.6, Eto Denki Co.). The schematic diagram of the ohmic heating circuit was showed in Fig. 3-3. Due to the characteristic of ohmic heating, the hot spot or areas inside sample during processing usually born in different materials and where received more electric field energies, we specified four points on the central vertical cross section of sample for verification as shown in Fig. 3-4.

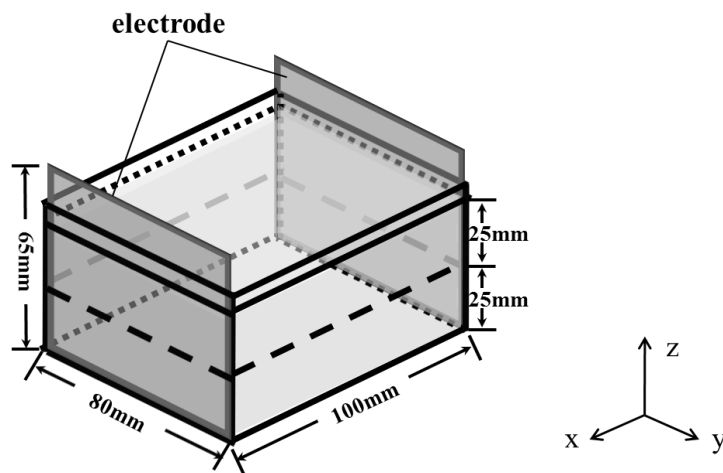


Fig. 3-1 The schematic of the static ohmic heating cell.

The parallel (parallel to electric current) and series model (perpendicular to electric current) imitated the laminar foods such as sandwich, hamburger and meat while the composite food at two typical surrounding-cases: pure-inside-salt model and salt-inside-pure model tending to point out the effect of location of ingredients with different electric conductivities on temperature distribution under ohmic heating. Both of them imitated ambient foods like egg and pie. In order to fill the ingredients more uniform, we prepared samples like Fig. 3-5 shown.

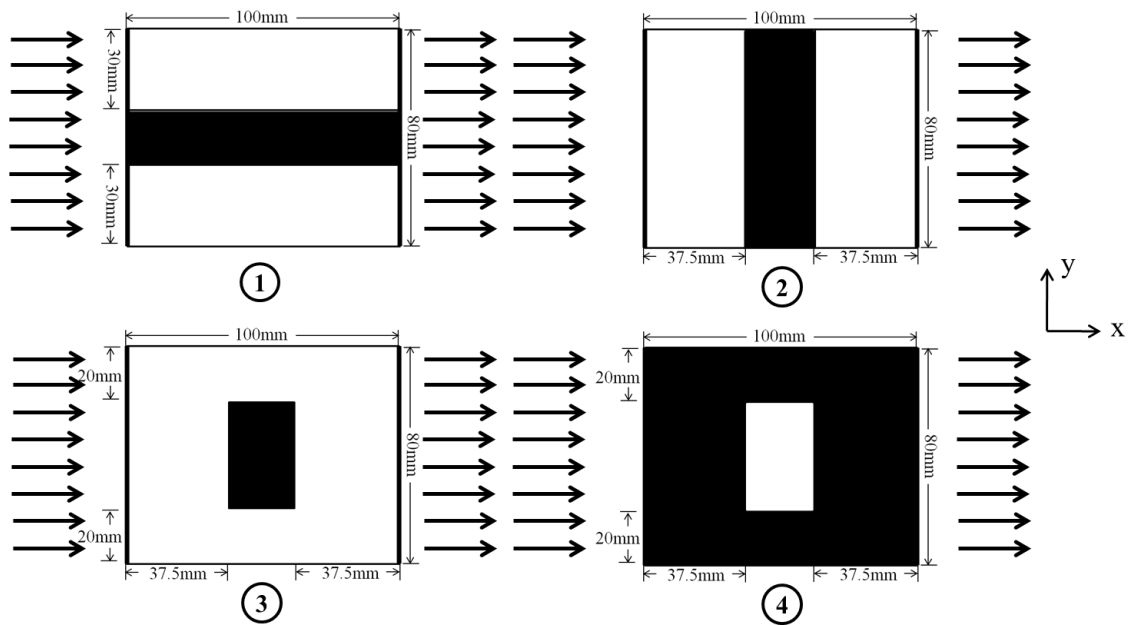


Fig. 3-2 The cross-sections of four filling patterns. (□ mashed potato with 1 wt % NaCl;

■ mashed potato; → the flow direction of electric current)

- ① parallel model (parallel to electric current);
- ② series model (perpendicular to electric current);
- ③ pure-inside-salt model;
- ④ salt-inside-pure model

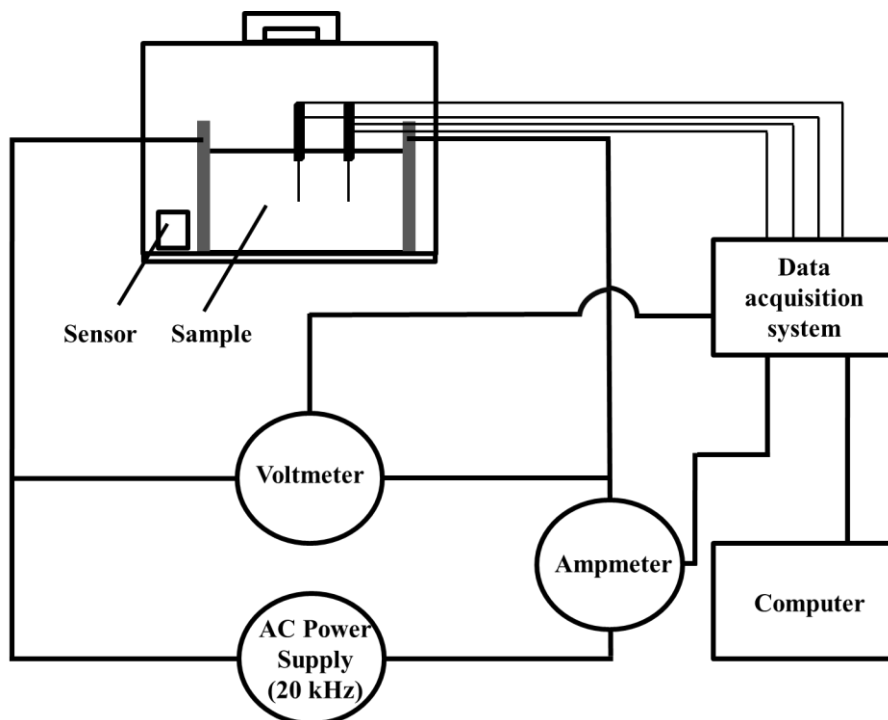


Fig. 3-3 The schematic diagram of the ohmic heating circuit.

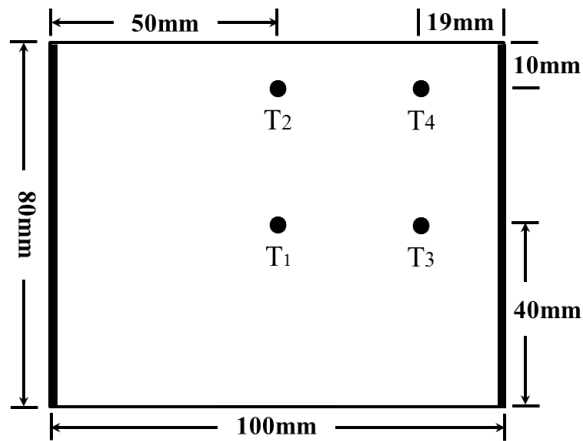


Fig. 3-4 The location of thermocouples from the top view for measuring temperature during ohmic heating.

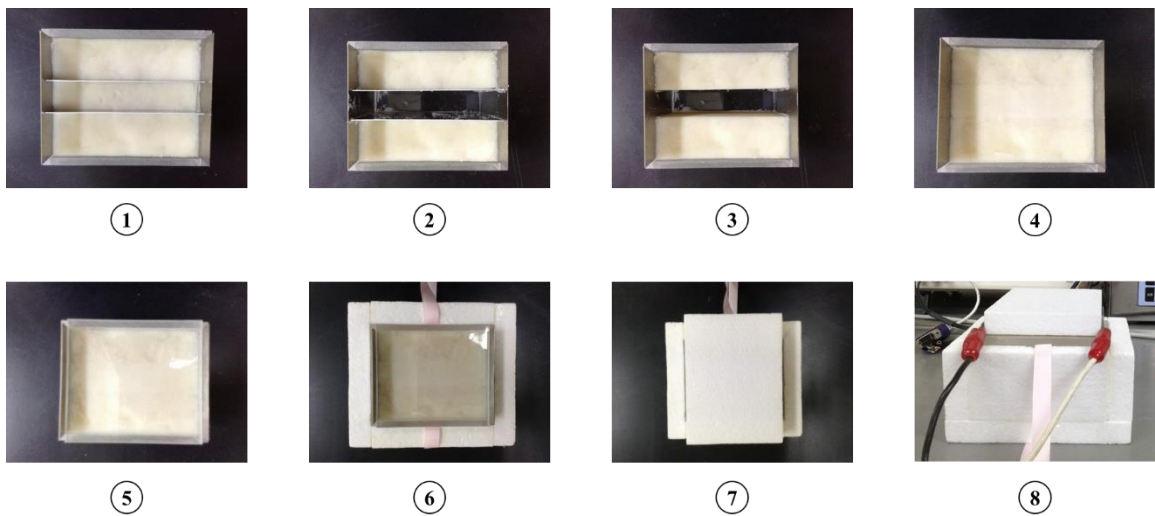


Fig. 3-5 The schematic of the filling method (using parallel model as an example).

- ① fill the cell with electrode and salted mashed potato, then insert the iron plate according to the parallel model;
- ② dig out the center part of the salted mashed potato;
- ③ pull out the iron plate;
- ④ fill the center part with pure mashed potato;
- ⑤ cover the lid;
- ⑥ put into the foam-plastic container and set the pulling rope in the middle;
- ⑦ cover the foam-plastic lid
- ⑧ finished

Temperature distributions of four typical filling patterns undergoing ohmic heating were investigated. These four patterns were designed with respect to the parallel, series and two typical surrounding-cases (pure-inside-salt model and salt-inside-pure model) when connected with electrodes as shown in Fig. 3-6. Then they were heated for certain time (in case①, ②, ③): 300s; in case ④): 600s). The temperature was monitored before the experiment started in order to obtain uniform initial temperature conditions $25 \pm 0.5^\circ\text{C}$ after calibration. Voltage and current were also continuously recorded at 1 s intervals during the experiment using multimeter  by a software , respectively. And the cell was cut into two parts equally in height (each of them is 25 mm in inner), the temperature distribution on horizontal cross sections after heating was quickly captured with an infrared thermal camera (TH5104; NEC san-ei Instruments, Ltd., Japan). These thermal graphs were then used to verify the simulated results by displaying with the same color labels.

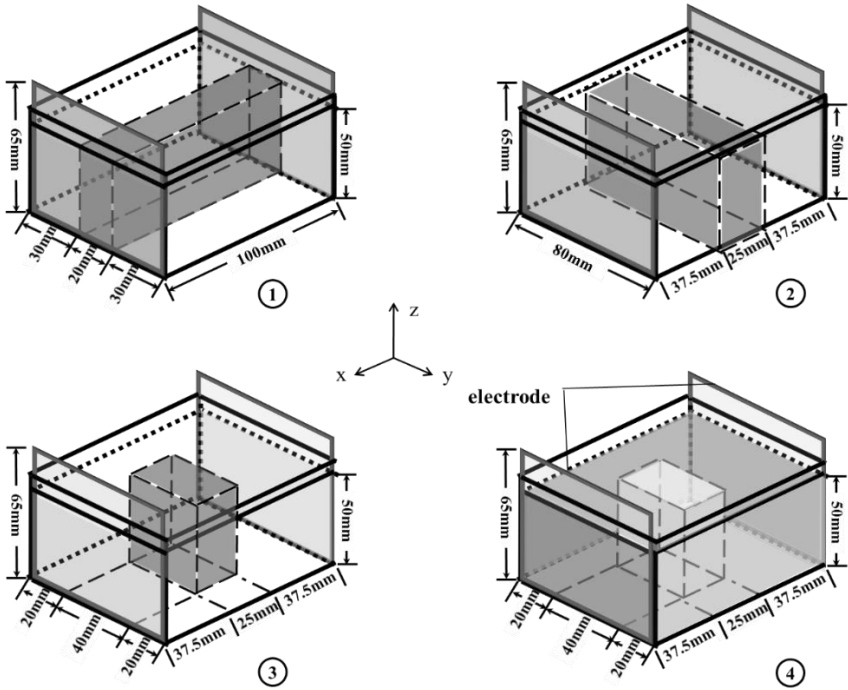


Fig. 3-6 The three dimensional model of four filling patterns.

- mashed potato with 1 wt % NaCl ■ mashed potato;
- ① parallel model (parallel to electric current);
- ② series model (perpendicular to electric current);
- ③ pure-inside-salt model;
- ④ salt-inside-pure model

3.3 Validation of ohmic heating machine

The 100 mM potassium chloride standard solution was used to validate the true output voltage of ohmic heating machine. 1 L KCl solution was poured into the static ohmic heating cell (100 ×100 ×100 mm) with two titanium plate electrodes (thickness is 2 mm) inserted the parallel internal wall of cell. Connected the multimeter parallel with the static ohmic heating cell (Fig. 3-7) then turned on the ohmic heating machine to apply the voltage with 20 kHz and adjusted the voltage output from 0-120 V of ohmic heating machine, when the ohmic heating showed 64.8 V, the value of mulimeter was 50 V.

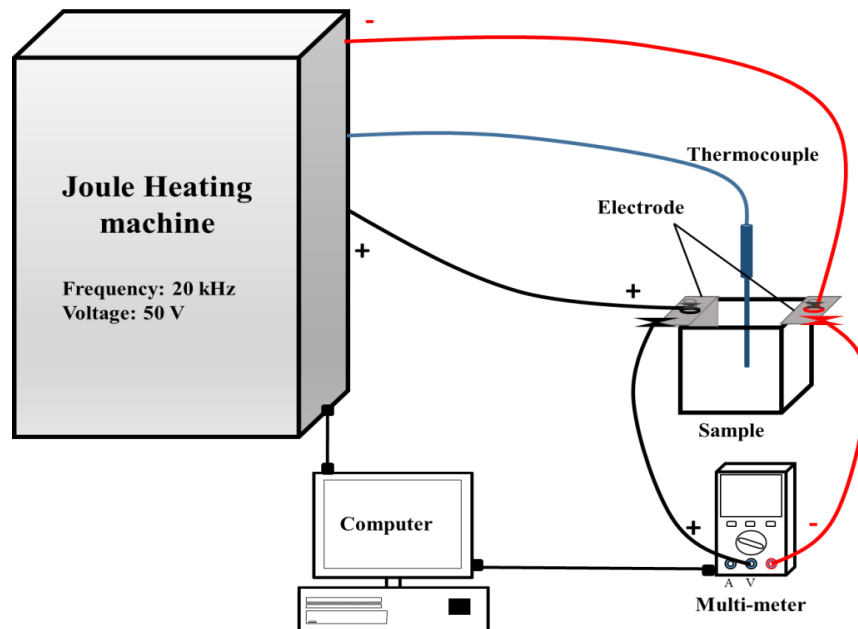


Fig. 3-7 Apparatus for measuring the real voltage of ohmic heating (parallel).

As can be seen from Fig. 3-8, the display of ohmic heating machine was lower than the real voltage measured by multimeter. And there is a linear relationship between them. Using this relation, we can get the true voltage applied to samples.

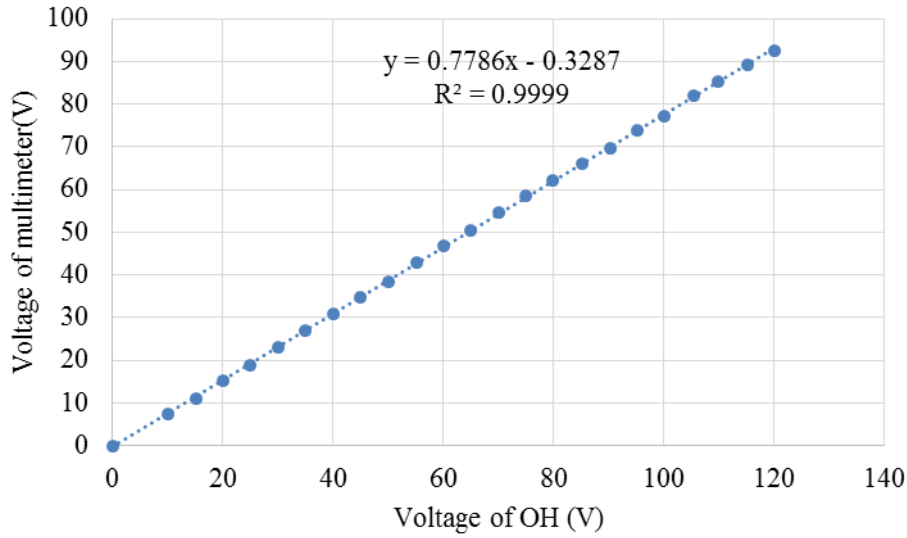


Fig. 3-8 The relationship between voltage of multimeter and ohmic heating.

In the same manner, connected the multimeter series with the static ohmic heating cell (Fig. 3-9) to adjust and measure the current passed through. We could easily conclude from Fig. 3-10 that the current displayed by ohmic heating machine significantly deviate from the real value. On the other hand, there was about 0.3 A difference between multimeter and V_m / R_{LCR} . This difference may be caused by the multimeter which was no exact accuracy at 20 kHz.

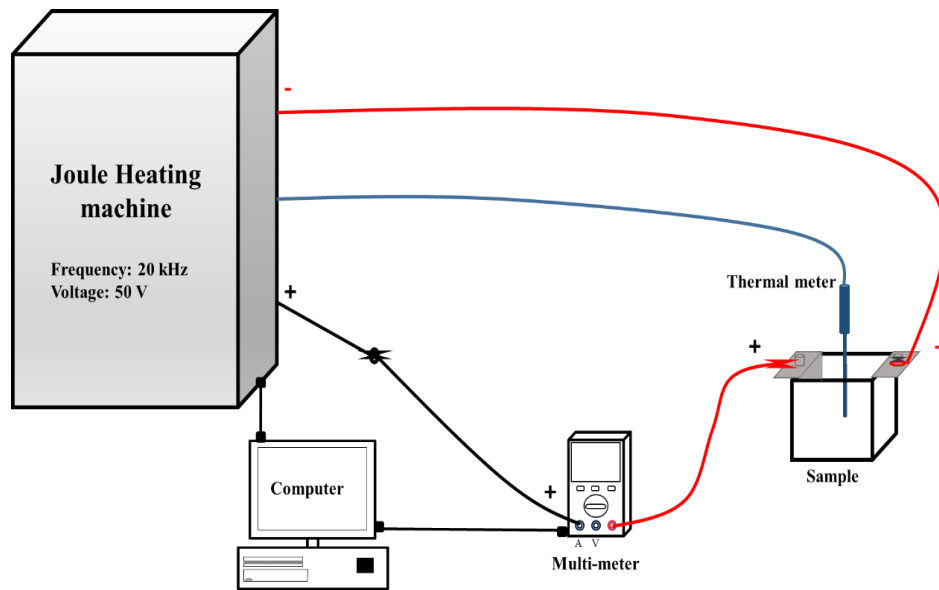


Fig. 3-9 Apparatus for measuring the real current of ohmic heating (series).

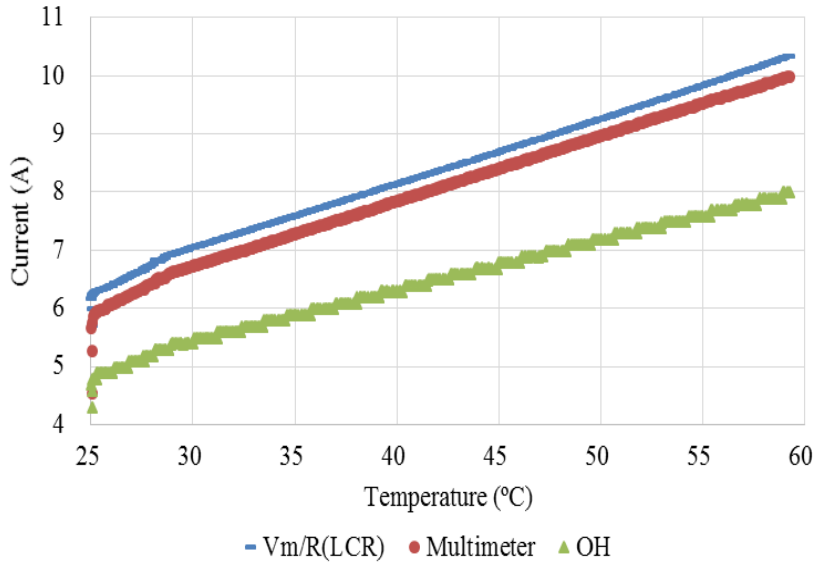


Fig. 3-10 The current of ohmic heating using different methods.

3.4 Check of heat generation of ohmic heating machine

With the same experimental condition of 3.3, whereas 100 mM KCl standard solution (1 L), mashed potato (990 g) and mashed potato with 1 wt % NaCl (990 g) were used. The temperature in the center measured by thermocouple was used to calculate heat generation. When the temperature increased 10 °C from initial heating was stopped. At the same time, the real voltage and current were recorded by multimeter and ohmic heating machine meter. The impedance of samples at certain temperature was also measured by LCR meter every 5 °C using LCR meter from 20 to 35 °C and used to calculate the total work as one method. Finally, we compared heat generation value with the total work to verify the results using Eqs as follow:

$$Q = Cm\Delta T \quad (3-1)$$

$$W_m = \Sigma V_m I_m t \quad (3-2)$$

$$W_{LCR} = \Sigma \frac{V_m^2 t}{R_{LCR}} \quad (3-3)$$

Where Q is the calorific value (J), C is specific heat ($\text{J kg}^{-1} \text{ }^\circ\text{C}^{-1}$), assumed that is 4.2×10^3 of all the samples, m represents mass of sample (kg), ΔT the change of temperature ($^\circ\text{C}$), t is the time (s), W_m the total electrical work calculated from the voltage (V_m) and current (I_m) value

from multimeter (J), W_{LCR} the total electrical work calculated from the resistance value from LCR meter (R_{LCR}).

As been shown by Table 3-2, both of the total work calculated from multimeter and LCR meter were near to that of heat generation. In the case of 100 mM KCl solution, among the three values, the heat generation was lowest that may due to the heat loss which occurred between the samples and environment.

Table 3-2. The comparison of total work and heat generation

Material	Q (J)	W_m (J)	W_{LCR} (J)	$\frac{Q}{W_m}$ (%)	$\frac{Q}{W_{LCR}}$ (%)
100 mM KCl	42126	44957	47335	93.7 %	89.0 %
Mashed potato	41580	36025	36738	115.4 %	113.2 %
Mashed potato with 1 wt % NaCl	41538	41004	44859	101.3 %	92.6 %

On the contrary, the heat generation was highest in the case of mashed potato because that ohmic heating is internally generated due to electrical resistance, which may cause the non-uniform of temperature and temperature highest in the center of the mashed potato where was solid food that has a low electrical conductivity. As to mashed potato contained 1 wt% NaCl, the electrical conductivity of it was about five times larger than that of mashed potato which means it would be easier for the current to pass through. Therefore, the results of salted mashed potato were similar with that of KCl solution.

3.5 Results and discussion

From the thermograph and isothermal line of parallel situation undergoing ohmic heating (Fig. 3-11), it was clearly that the temperature was lower in the middle where mashed potato was filled. In this parallel condition, the current is easier to pass through the material which has

a higher electric conductivity. At this point, the current density inside the salted mashed potato is much more intensive leading to higher temperature. On one hand, the highest temperature 56 °C appeared in the center inside the salted mashed potato, and the temperature decreased from center to outside. This phenomenon occurred because the heat was generated internally due to the resistance of material during ohmic heating. On the other hand, the lowest temperature 35 °C appeared at begin and end inside mashed potato.

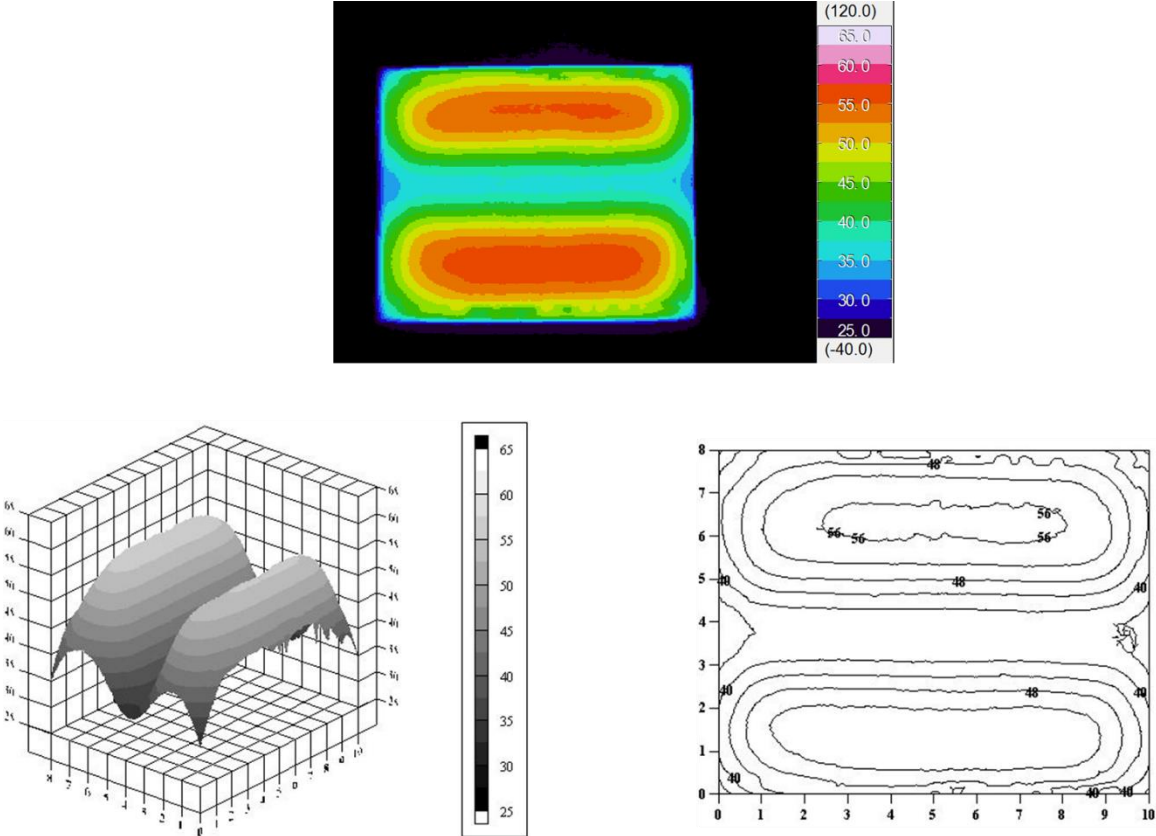


Fig. 3-11 The temperature distribution of center horizontal cross section undergoing 300s ohmic heating processing of parallel situation. (top: thermograph; left: stereo isothermal line ; right: isothermal line)

The temperature histories of four points in the middle height were shown in Fig. 3-12 and Fig. 3-13. Both of point 2 and 4 were measured in salted mashed potato and showed much more rapid increasing rate of temperature compared with point 1 and 3 which were put into mashed potato. In the same material, there was no significant difference in ending temperature and

increasing rate of temperature. The difference of ending temperature in two different components which exposed in the same electrical field strength in this system was 23 °C. It emphasized the importance of electric conductivities of each component in food system during ohmic heating.

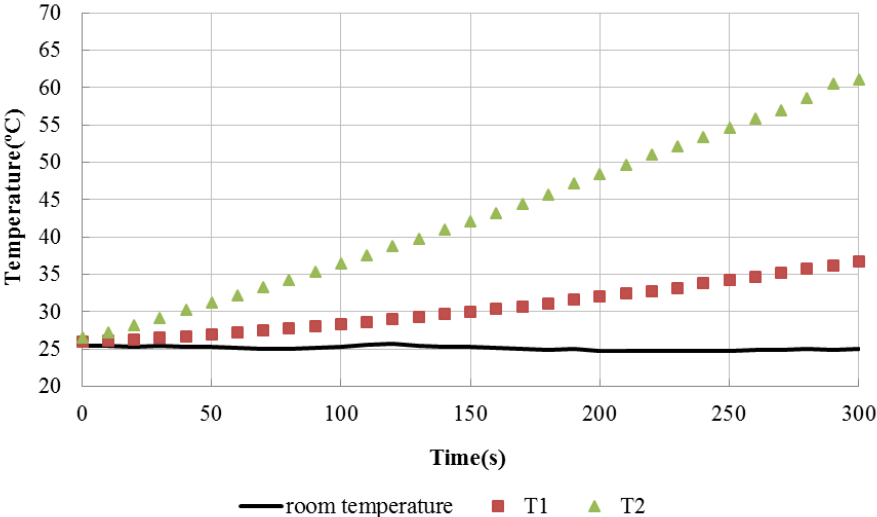


Fig. 3-12 The temperature history of point 1 and point 2 during ohmic heating processing of parallel situation.

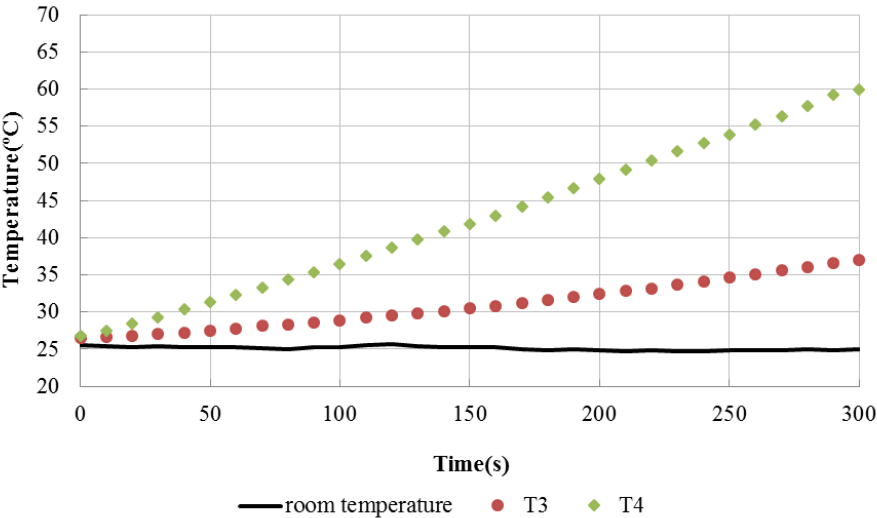


Fig. 3-13 The temperature history of point 3 and point 4 during ohmic heating processing of parallel situation.

In contrast, the temperature is higher in the middle where mashed potato was filled in series condition (Fig. 3-14). These phenomena due to the whole current pass through each ingredient are same in series circuit; while mashed potato has bigger impedance resulted in the higher temperature. 60 °C, the highest temperature, appeared in the center of and then decreased from center to the outside of the whole system. In mashed potato, the temperature appeared as an annular temperature range. And centered on it, outside temperature showed strict decreasing trend with arcuate temperature band. The lowest temperature was in outermost layer at 30 °C.

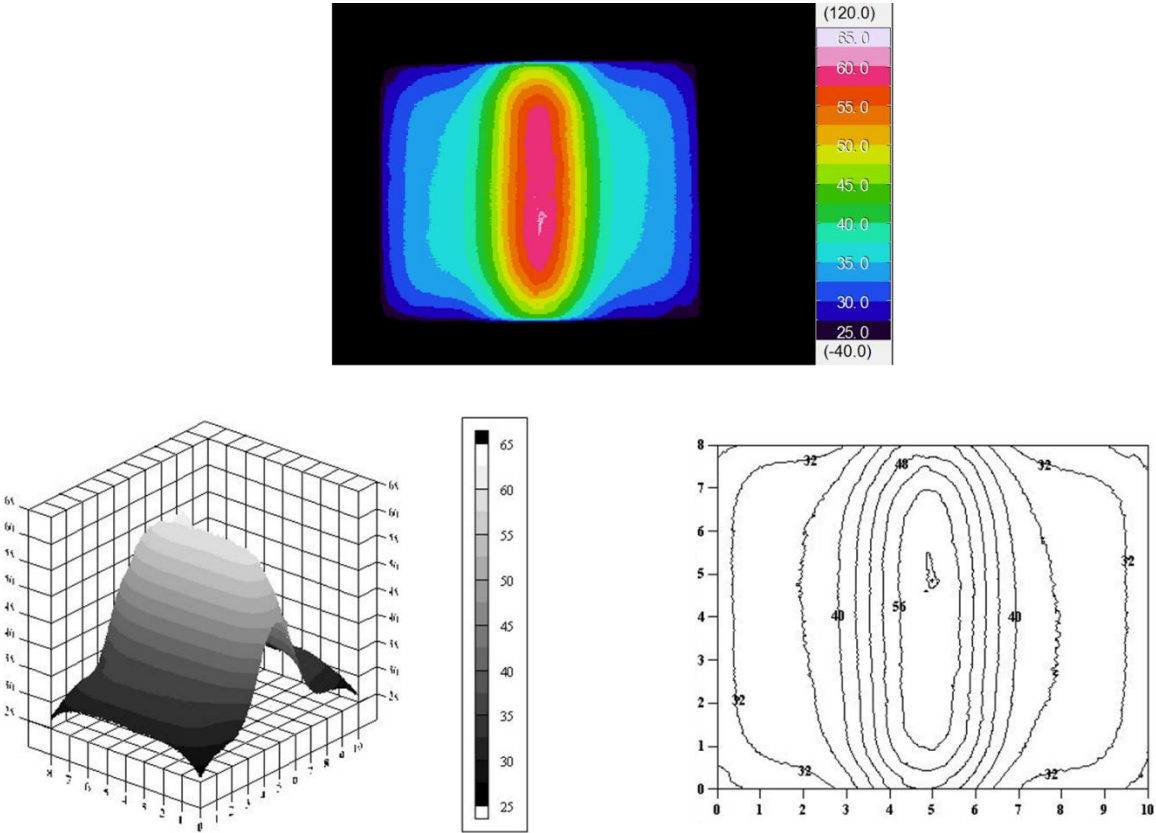


Fig. 3-14 The temperature distribution of center horizontal cross section undergoing 300s ohmic heating processing of series situation. (top: thermograph; left: stereo isothermal line ; right: isothermal line)

From Fig. 3-15 and Fig. 3-16, the ending temperature of point 1 and 2 measured in mashed potato were about 26 °C higher point 1 and 3 which were put into mashed potato. In the same material, the temperature of point 1 was apparently higher than point 2 due to the center location

of point 1 and the internal heating specialty of ohmic heating.

Besides, when compared temperature distribution with parallel situation, the completely opposite effect was found. It was easy to find the conclusion that the arrangement conditions of materials have a significant influence on the temperature distribution during ohmic heating. Components connected in parallel are connected so the same voltage is applied to each component. In a parallel circuit, the voltage on each of the components is the same, and the total current is the sum of the currents through each component. In a series circuit, the current through each of the components is the same, and the voltage across the circuit is the sum of the voltages across each component.

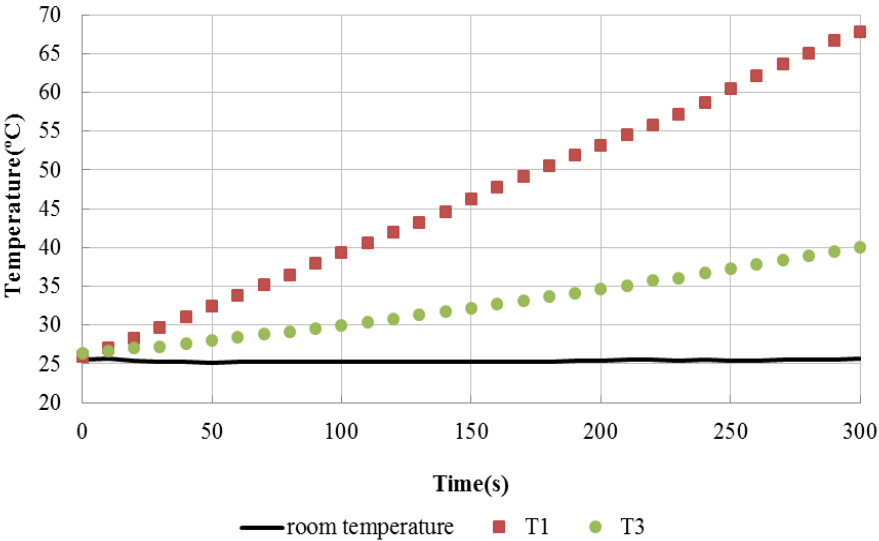


Fig. 3-15 The temperature history of point 1 and point 3 during ohmic heating processing of series situation.

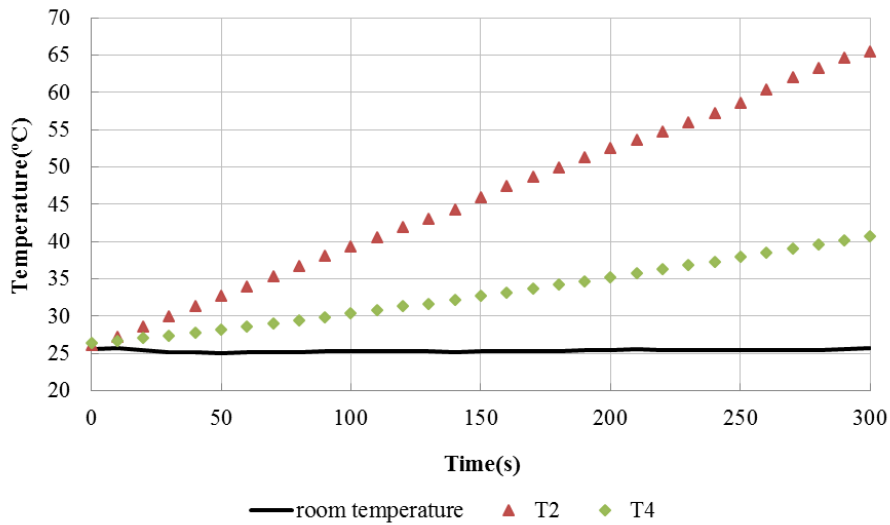


Fig. 3-16 The temperature history of point 2 and point 4 during ohmic heating processing of series situation.

In the pure-inside-salt situation (Fig. 3-17), we found that the temperature inside sole component of salted mashed potato was no longer uniform. The temperature centralized at the locations in the top and bottom of mashed potato. It was due to the relatively bigger impedance of the mashed potato in the middle of this situation that restricts the flow of current. The salted mashed potato with higher electric conductivity is much easier for current to pass through. The current passed through salted mashed potato smoothly, then run up against mashed potato which has a low electric conductivity where was difficult for current to pass through. So the current tended to change the route to keep away from mashed potato. Electrical current density centralized highly at the top and bottom of mashed potato that resulted in highest temperature of 70 °C. The temperature decreased from this point to outside. Cold spot below 40 °C occurred in front and at the back of mashed potato.

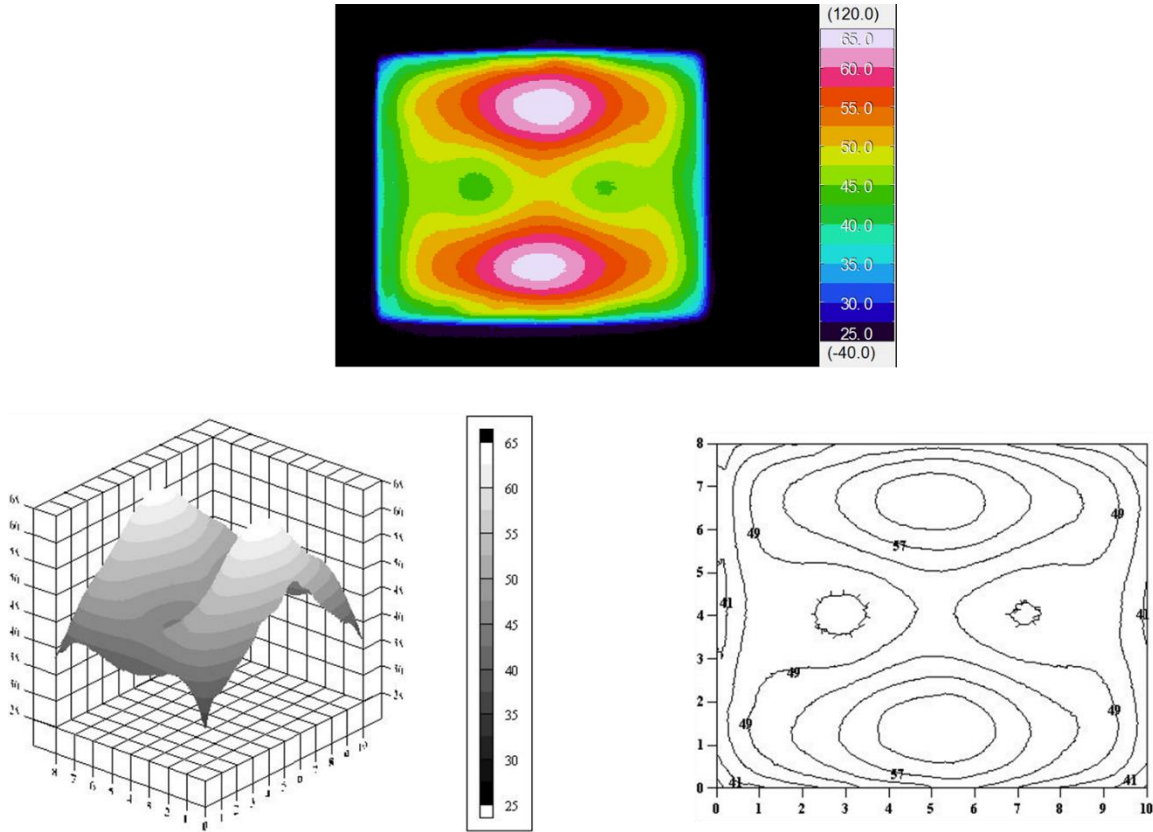


Fig. 3-17 The temperature distribution of center horizontal cross section undergoing 300s ohmic processing of pure-inside-salt situation. (top: thermograph; left: stereo isothermal line ; right: isothermal line)

From Fig. 3-18 and Fig. 3-19, the ending temperature of point 2 (70 °C), 3 (40 °C) and 4 (55 °C) measured in salted mashed potato has a significant difference due to the existence of mashed potato in the center. Inside mashed potato, the temperature was about 50 °C owing to the low electric conductivity.

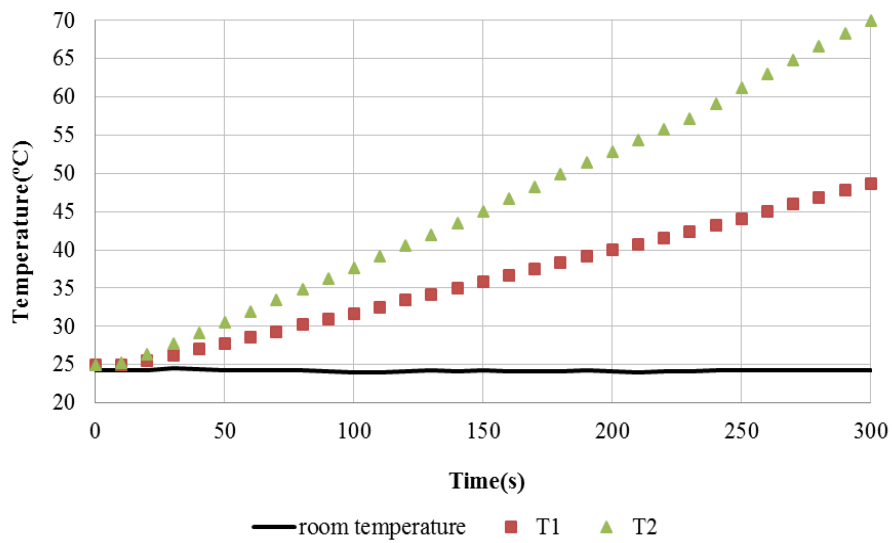


Fig. 3-18 The temperature history of point 1 and point 2 during ohmic heating processing of pure-inside-salt situation.

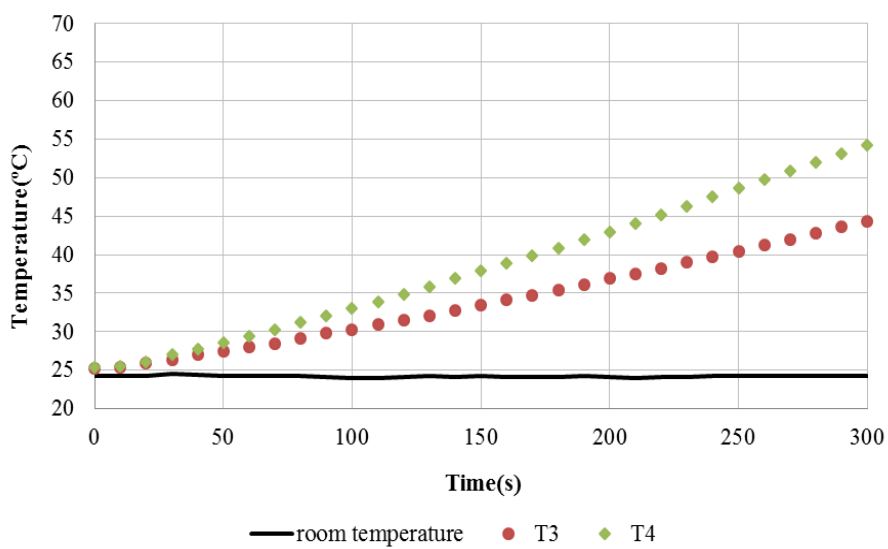


Fig. 3-19 The temperature history of point 3 and point 4 during ohmic heating processing of pure-inside-salt situation.

In the salt-inside-pure situation, the majority of the composite food is mashed potato with low electric conductivity. After 300 s ohmic heating processing, the whole temperature of the cross-section is so low that we cannot distinguish the distribution very well. As a result, we added the heating time to 600 s. From this result (Fig. 3-20), we found that the temperature distribution appeared funnel shape because of the current tending to centralize into the middle where was easy to pass through. In the salted mashed potato, the temperature was about 35 °C which was lower than that of mashed potato around it due to the low impedance it has. Hence, the highest temperature 44 °C appeared in front and at the back of the salted mashed potato. The lowest temperature was in outermost layer at 30 °C.

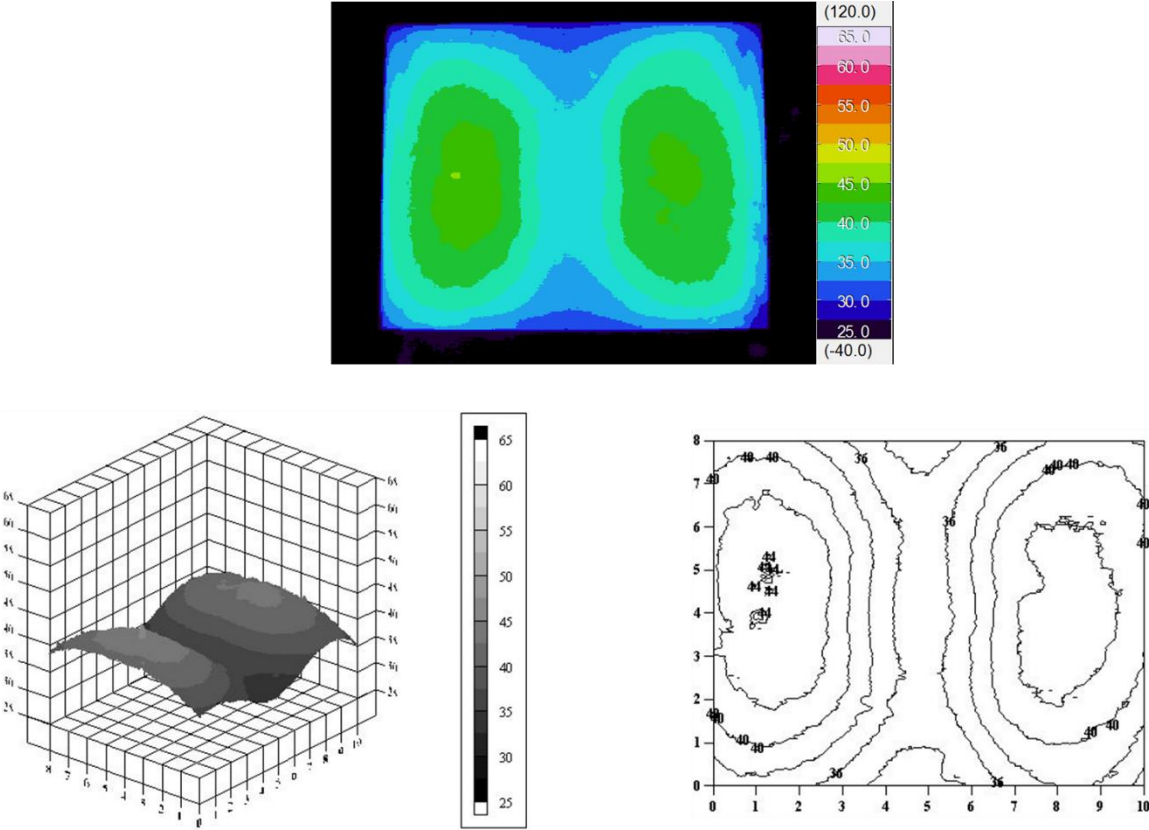


Fig. 3-20 The temperature distribution of center horizontal cross section undergoing 600 s ohmic heating processing of salt-inside-pure situation. (top: thermograph; left: stereo isothermal line ; right: isothermal line)

From Fig. 3-21 and Fig. 3-22 of salt-inside-pure situation, the ending temperatures of all the four points were lower than that of other situation while the electrical field strength applied was same. The temperature of point 3 was highest at 48 °C while in thermograph it was 44 °C. The temperature of thermograph was lower than temperature measured by thermocouple, because sample was exposed in the environment at 25 °C resulted in temperature difference and the heat loss was occurred when the sample cut into two part to get the thermograph. We also noted that in mashed potato the ending temperature were different at point 2 (35 °C), 3 (48 °C) and 4 (41 °C).

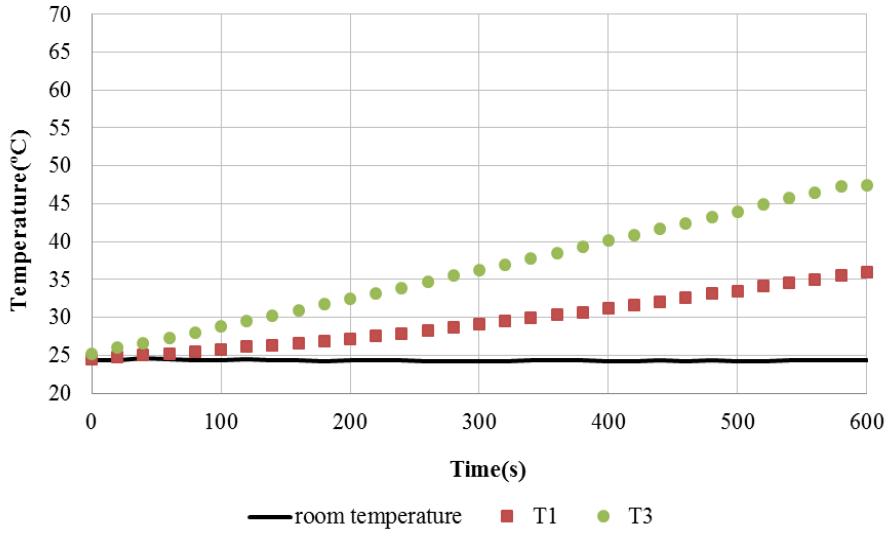


Fig. 3-21 The temperature history of point 1 and point 3 during ohmic heating processing of pure-inside-salt situation.

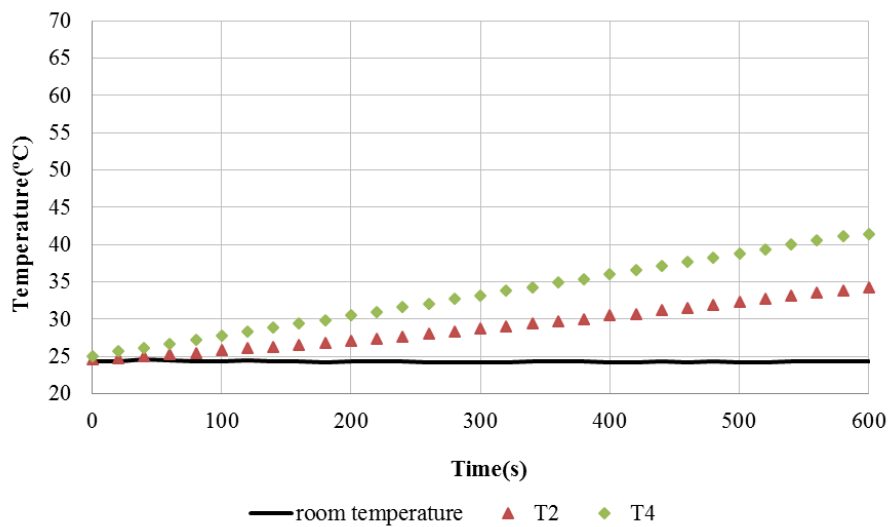


Fig. 3-22 The temperature history of point 2 and point 4 during ohmic heating processing of pure-inside-salt situation.

3.6 Conclusion

The electric conductivity was the key factor which influenced the current distribution inside food during ohmic heating. It increased along with the growth of salt concentration explained by the less impotent opposition to the movement of the ions for higher temperature. In sole component situation, the current was easy to pass through the material with high electric conductivity. In contrast, the material with low electric conductivity has a higher impedance resulted in more heat generated performed as high temperature.

Different components and their arrangement conditions were observed to have a significant influence on the temperature distribution during ohmic heating. In parallel, the temperature was lower in the middle where filled with mashed potato because it was easier for current to pass through the ingredient with a higher electric conductivity. In contrast, the temperature was higher in mashed potato in series connection. This phenomenon can be explained using Joule's Law. Otherwise, in salt-inside-pure and pure-inside-salt condition, the phenomenon was much more complex that needed the knowledge of the electrical field distribution. Even in the same

component, the temperature was not uniform due to the existence of other component and its location which influenced distributions of the electrical field.

To sum up, the electric conductivity of each component is the main factor which influences the temperature distribution and if the electrodes locate at the regular direction, the arrangement of component also has a significant effect on the temperature distribution in composite solid food system during ohmic heating.

3.7 Reference

Filiz Icier., & Coskan Ilicali. (2005). Temperature dependent electrical conductivities of fruit purees during ohmic heating. *Food Research International*, 38, 1135-1142.

JaeYong Shim., Seung Hyun Lee., Soojin Jun. (2010). Modeling of ohmic heating patterns of multiphase food products using computational fluid dynamics codes. *Journal of Food Engineering*, 99, 136-141.

L.J. Davies., M.R. Kemp., P.J. Fryer. (1999). The geometry of shadows: effects of inhomogeneities in electrical field processing. *Journal of Food Engineering*, 40, 245-258.

Markus Zell., James G. Lyng., Denis A. Cronin ., Desmond J. Morgan. (2009). Ohmic heating of meats: Electrical conductivities of whole meats and processed meat ingredients. *Meat Science*, 83, 563-570.

Markus Zell., James G. Lyng., Denis A. Cronin ., Desmond J. Morgan. (2010). Ohmic heating of whole turkey meat- effect of rapid ohmic heating on selected product parameters. *Food Chemistry*, 120, 724-729.

N. Shirsat., J.G. Lyng., N.P. Brunton., B. McKenna. (2004). Ohmic processing: Electrical conductivities of pork cuts. *Meat Science*, 67, 507-514.

S.K. Sastry., & S. Palaniappan. (1992). Mathematical modelling and experimental studies on ohmic heating of liquid-particle mixtures in a static heater. *Journal of Food Process Engineering*, 15 (4), 241-261.

S.M. Zhu., M.R. Zareifard., C.R. Chen., M. Marcotte.,S. Grabowski. (2010). Electrical conductivity of particle-mixtures in ohmic heating: Measurement and simulation. *Food Research International*, 43, 1666-1672.

- S. Salengke., & S.K. Sastry. (2007). Experimental investigation of ohmic heating of solid-liquid mixtures under worst-case heating scenarios. *Journal of Food Engineering*, 80, 324-336.
- Wadad G. Khalaf., & Sudhir K. Sastry. (1996). Effect of viscosity on the ohmic heating rate of solid-liquid mixtures. *Journal of Food Engineering*, 27, 145-158.
- Wassama Engchuan., Weerachet Jittanit., Wunwiboon Garnjanagoonchorn. (2014). The ohmic heating of meat ball: Modeling and quality determination. *Innovative Food Science and Emerging Technologies*, 23, 121-130.
- W.-R Fu., & C.-C Hsieh. (1999). Simulation and verification of two-dimensional ohmic heating in static system. *Journal of Food Science*, 64 (6), 946-949.
- Xiaofei Ye., Roger Ruan., Paul Chen., Christopher Doona. (2004). Simulation and verification of ohmic heating in static heater using MRI temperature mapping. *Lebensm.-Wiss. u.-Technol*, 37, 49-58.
- Y. Benabderrahmane., & J.-P. Pain. (2000). Thermal behaviour of a solid/liquid mixture in an ohmic heating sterilizer- slip phase model. *Chemical Engineering Science*, 55, 1371-1384.

Chapter 4- Modeling of ohmic heating of solid food

4.1 Introduction

It is well known that higher temperature and longer heat exposure time normally lead to the quality deterioration of food product. Ohmic heating is an emerging thermal processing technique with large number of actual and future application that has potential to prevent them. It is a rapid heating method and has been suggested to be much uniform than other electroheating techniques. Such a rapid heating rate involves a high electric power to be dissipated, which makes the process very sensitive to the electric field distribution.

Different ohmic heating chamber designs have been proposed over the years, mainly with co-linear, co-liner, co-axial and parallel electrode configurations (Mykola Shynkary and Sudhir K. Sastry, 2010). It has been shown that the non-uniform temperature distribution can be compensated by geometry adjustment and achieving a turbulent flow which provides an effective mixing. S.M. Zhu *et al.*, (2010) compared the measured and predicted temperature profiles in various solid-fluid structural systems considering five theoretical models (series, parallel, two forms of Maxwell-Eucken models and effective medium theory). Regardless of the diversity of designs, little information is available about electric field and temperature distribution of solid food during treatment. And the calculations of changing product temperature and subsequently required heating-up time for the ohmic heating process are quite complicated and not completely studied. It can be related to the complexity of the process that makes experimental study very difficult. Recent works by the present research group have led to the development of meat preparation protocols which largely satisfy the latter requirement and to a mathematical model prediction cold regions (Markus Zell *et al.*, 2009; 2010). Based on these preliminary studies it was apparent that modeling of temperature distribution was essential in order to clarify the mechanism of heat generation of multi-component foods in theory and optimize the processing method. In particular, depending on the multi-components in composite solid food with different thermal properties can be substantial resulting in unacceptably high temperature gradients within the product which in turn can have quality and safety implications.

On the other hand, extensive development of numerical simulation software and computers' computing power rise during the past decades has allowed for successful simulation of ohmic heating. Numerical simulation is based on solving the governing equations describing the process under investigation. F. Marra *et al.*, (2009) pointed out that the mathematical model of the ohmic heating should be developed to quantify heat losses and to evaluate the influence of main factors on the product temperature during thermal processing. There are number of reports where food electrical treatment was successfully simulated with FEM software. Soojin Jun and Sudhir Sastry (2007) also performed a three-dimensional model for heat transfer to predict the heating patterns of tomato soup inside the pouch under ohmic heating. Xiaofei Ye *et al.*, (2004) simulated ohmic heating of liquid-particulate mixtures in a static heater with parallel electrodes used FEMLAB. Extra computational work based on Joule heating effect which needed to determine distortion of electric current resulted in the temperature distribution for both solid and liquid phases was published (W.-R. Fu and C.-C.Hsieh, 1999). The effects of ohmic heating on electrokinetic transport of solutes also described by the comprehensive 3D mathematical models including Poisson-Boltzmann equation, Laplace equation, modifying Navier-Stokes equation, energy equation and mass transport equation using the finite volume based on CFD technique (Gongyue Tang *et al.*, 2007).

Despite some studies in the area of mathematical model development for predicting the product temperature during ohmic heating process as mentioned above, not much attention has been given to addressing cold-spots identification and the measurement during complex foods processing and modeling especially for multi-component foods during ohmic heating. Therefore understanding, characterizing and modeling of temperature distribution in solid food during ohmic heating is required in order to optimize and possibly exploit.

According to the reasons mentioned above, the objectives of this study were to establish a fully three-dimensional (3D) finite element models based on Maxwell's equation by coupling the analysis of electrical field, heating generation and heat transfer for predict the temperature distributions of four typical solid composite food systems: the parallel (parallel to electric current) and series model (perpendicular to electric current) and two typical surrounding-cases:

pure-inside-salt model and salt-inside-pure model during ohmic heating. And all simulations were finally validated by the experiment at a selected set of representative locations. And were optimized with high accuracy.

4.2 Material and Methods

As well known, electromagnetic induction is the production of a potential voltage across a conductor when it is exposed to a varying magnetic field. That is, the electric and magnetic fields are not completely separate phenomena. For this reason, a new method of predicting the heat generation inside the food undergoing ohmic heating based on electromagnetic field analysis using Maxwell's equations was proposed instead of Joule's law, which showed the potential of applying the commercial software packages that were designed for electromagnetic field and temperature analysis for temperature predicting undergoing ohmic heating.

4.2.1 Governing equations

4.2.1.1 Heat generation based on Maxwell's equations

Electromagnetic field distribution in space and time is governed by Maxwell's equations which describe how electric charges and electric currents act as sources for the electric and magnetic fields and how they affect each other to calculate the current distribution. The differential form of Maxwell's equations could be expressed in terms of electric field and magnetic intensity (E and H), as follows (Knoerzer et al., 2008; Chandrasekaran *et al.*, 2011):

$$\nabla \cdot B = \nabla \cdot \mu H = 0 \quad (4-1)$$

$$\nabla \cdot D = \nabla \cdot \varepsilon E = \rho_m \quad (4-2)$$

$$\nabla \times H = \frac{\partial D}{\partial t} + J = \frac{\partial \varepsilon E}{\partial t} + \sigma E \quad (4-3)$$

$$\nabla \times E = -\frac{\partial B}{\partial t} = -\frac{\partial \mu H}{\partial t} \quad (4-4)$$

$$\sigma = \omega \varepsilon_0 \varepsilon'' \quad (4-5)$$

Where B is magnetic induction (Wb m^{-2}), D is electric displacement (C m^{-2}), and H (A m^{-1})

¹⁾ and E (V m^{-1}) are the magnetic field and electric field intensity. ρ_m is the electric volume charge density (As m^{-3}), J is current flux (A m^{-2}), ε is the complex permittivity ($\varepsilon = \varepsilon' - j\varepsilon''$ with $j^2 = -1$), and the permeability μ could be represented by $\mu_0 = 4\pi \times 10^{-7}$ (H m^{-1}), the magnetic permeability of free space. The electric conductivity σ is related to the relative dielectric loss factor of the material (ε''), where ω ($\omega = 2\pi f$, f stands for the frequency) is the angular frequency (rad s^{-1}), and $\varepsilon_0 = 8.854 \times 10^{-12}$ (F m^{-1}) is the permittivity of free space.

The internal volumetric heat generation term could be then estimated using Eq. (4-6) (Birla *et al.*, 2008) after electromagnetic field analysis:

$$Q(x, y, z, t) = \omega \varepsilon_0 \varepsilon'' E^2 = \sigma |E|^2 \quad (4-6)$$

$$\rho C_p \frac{\partial T}{\partial t} = \nabla(k \nabla T) + Q_{gen} \quad (4-7)$$

With the heat generation data, the spatial and transient temperature were then calculated using Fourier's heat transfer equation expressed as Eq. (4-7) (Whitaker, 1977). The mass transfer was neglected in this simulation as the temperature at the end of heating stayed at a low level.

4.2.1.2 Equations of Joule's law

In plasma physics, the ohmic heating needs to be calculated at a particular location in space. The differential form of ohmic heating equation gives the power per unit volume.

$$P = J \cdot E \quad (4-8)$$

A basic and general definition starts from the fact that if there is electric field inside a material, it will cause electric current to flow. The electrical conductivity is defined as the ratio of the density of the current to the electric field:

$$\sigma = \frac{J}{E} \quad (4-9)$$

Using Eq. (4-9), Joule's law Eq. (4-8) is rewritten as

$$P = \sigma |E|^2 \quad (4-10)$$

4.2.1.3 The correlation of Joule's law and Maxwell's equations

From Eq. (4-6) and (4-10), we can easily find that the internal volumetric heat generation term is equal to the power per unit volume in numerical value. Above all, we can get the conclusion that Maxwell's equations can calculate the internal heat generation term undergoing ohmic heating in theory.

4.2.2 The model

Two commercial finite element methods based software packages, FEMAP (V10.2, Siemens PLM Software Inc., Plano, Texas, USA) and PHOTO-Series (V7.2, PHOTON Co. Ltd., Kyoto, Japan), were used. The three-dimensional geometric models were built by FEMAP corresponding to the real structure and size of experiments. The boundary conditions, electric intensity and the other parameters including dielectric and thermal properties of samples were set in PHOTO-Series, where the united analysis of electromagnetic field and heat transfer were carried out for temperature estimation.

4.2.2.1 Initial and boundary conditions

The start temperature of sample, container and surrounding air were set at room temperature (25 °C).

The boundary of the electrode surface was assumed perfect electrical conductors, where magnetic and electric field strength should be zero (Liu, *et al.*, 2013).

4.2.2.2 Assignment of power input

The current is transmitted inside the model along the x -direction and energy inside is distributed in the shape and could be assigned on the nodes of elements (Oomori, 1993; Liu *et al.*, 2013). The root mean square value of the electric field E_{rms} set in FEMAP could calculate

from the peak value of voltage using Eq. (4-11) (Marshall and Metaxas, 1998; Curet *et al.*, 2008).

$$E_{rms} = \frac{V_{peak}}{L} = \frac{\sqrt{2}V}{L} \quad (4-11)$$

4.2.2.3 Other conditions and input values

The negative value of dielectric loss factor that calculated from electrical conductivities determined experimentally would set in PHOTO-Series. Other properties for material A (mashed potato) and B (mashed potato with 1 wt % sodium chloride) are approximated by those of water, which is main constituent about 80 wt %, and the polypropylene properties were taken from Liu *et al.*, (2013). For the sample we used was mashed potato, and the thermal diffusivity of which was almost constant in the temperature range observed in this study (Fraile and Burg, 1997), the thermal properties was also assumed as constant. The initial temperature of heating system including sample and cell were also assumed homogeneous. The dielectric loss factor was calculated by the electric conductivities measured in Chapter 2. The distribution of heat generation was also considered to change significantly with heating time. Therefore, the temperature dependency of electric conductivity could not be neglected, and electromagnetic field should be analyzed and updated with dielectric loss factor depending on the influential factors mentioned above. Data inputs to the model are detailed in Table 4-1.

To get results with good accuracy, the converge test tolerance levels for the electromagnetic and temperature analyses were set at 1.0×10^{-8} and 1.0×10^{-12} , respectively. And the divergence tolerance and the maximum iterations for calculating were set at 1.0×10^{40} and 1.0×10^6 (Liu *et al.*, 2013a). The simulations were solved using Maxwell's equation, and the main solution steps have been introduced in Fig. 4-1.

Table 4-1. Summary of material properties and initial conditions used in the model.

Material	Value		
	Container	Mashed potato	Mashed potato with 1wt % sodium chloride
Initial temperature (T , °C)	25	25	25
Frequency (f , kHz)	20	20	20
Input electrical field ($V\ m^{-1}$)	-	707.1068	707.1068
Thermal conductivity (k , $W\ m^{-1}\ K^{-1}$)	1.900×10^{-1}	6.050×10^{-1}	6.050×10^{-1}
Density (ρ , $kg\ m^{-3}$)	1.200×10^3	1.042×10^3	1.042×10^3
Specific heat (C_p , $J\ kg^{-1}\ K^{-1}$)	1.464×10^3	4.180×10^3	4.180×10^3
Dielectric loss (ϵ'')	-8.988×10^{-9} (the value of air used in EM model)	$26.397T^2$ $-8246.7T-99362$ ($R^2=0.9966$)	$84.113 T^2$ $-30324T-621536$ ($R^2=0.9962$)

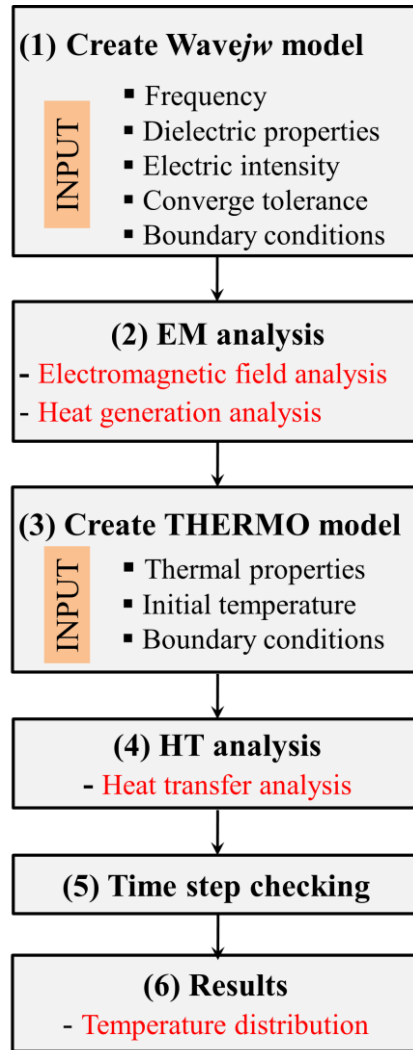


Fig. 4-1 The main solution steps for simulations.

4.3 Validation of model

Assume the circuit was pure resistor element circuit and the size was $100 \times 100 \times 100$ mm, $R_1=100 \Omega$, $R_2=50 \Omega$, $R_{air}=10^{18} \Omega$, $V=100$ V, $f=20000$ Hz, $t=1$ s.

We calculated the electrical work by Joule's Law using Eq. (4-12) and compared with heat generation predicting from software PHOTO-series for three conditions: (1) only R_1 in circuit; (2) R_1 and R_2 series connected in circuit (Fig. 4-2); (3) R_1 and R_2 parallel connected in circuit (Fig. 4-3). And the parameter needed to set into PHOTO was the minus of relative dielectric loss factor (ε'') and the root mean square value of the electric field (E_{rms}). The relative dielectric loss factor of the material is related to the electric conductivity σ as Eq. (4-5) shown, where ω

$= 2\pi f$, and $\epsilon_0 = 8.854 \times 10^{-12}$ (F m⁻¹). The root mean square value of the electric field was calculated using Eq.(5-11).

$$W = \frac{V^2 t}{R} \quad (4-12)$$

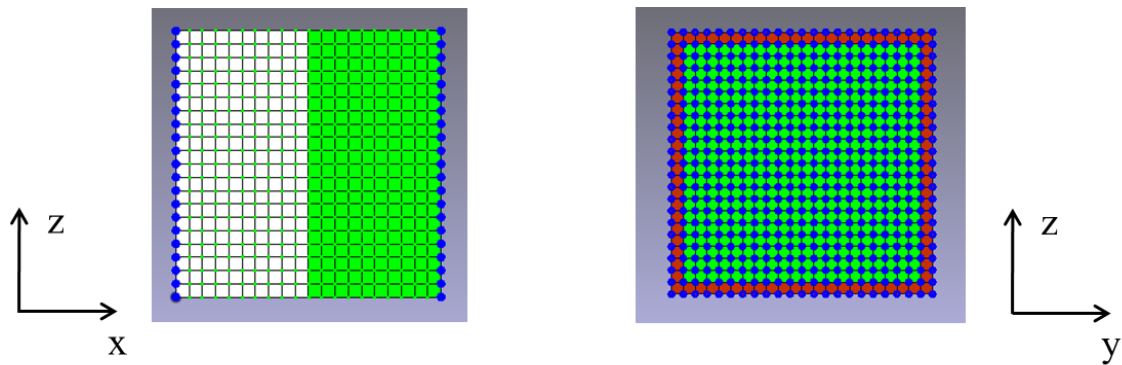


Fig. 4-2 The schematic diagram of series model in PHOTON (□ R_1 ■ R_2 ● electrode).

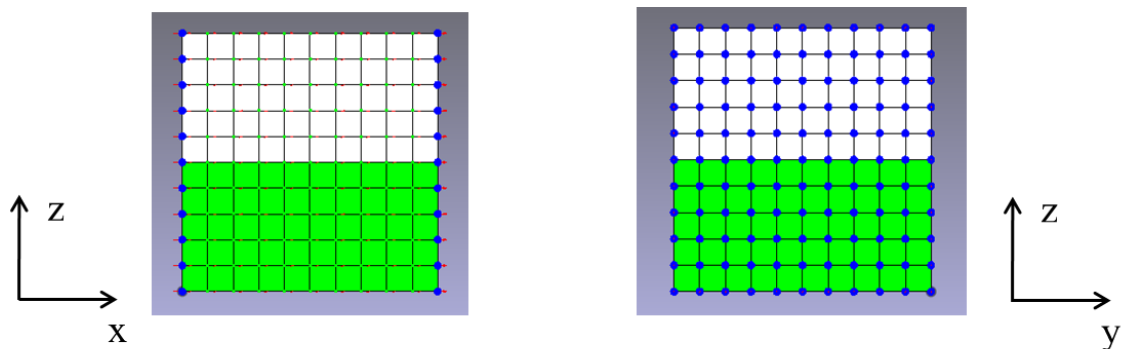


Fig. 4-3 The schematic diagram of parallel model in PHOTON (□ R_1 ■ R_2 ● electrode).

The calculated method and parameters need for both Joule's law and PHOTON were given in Table 4-2 and Table 4-3. The result of total work and heat generation were shown in Table 4-4. From the result, it was obvious that the total work calculated by Joule's law and the heat generation simulated using PHOTON software were almost the same in value of both series and parallel circuit. It identified the accuracy of PHOTON for calculation of heat generation and analysis of electromagnetic field by Maxwell's equation at certain condition.

Table 4-2. The method used in series and parallel circuit for total work by Joule's Law.

Circuit	$R_{total} (\Omega)$	W_1 & W_2
Series circuit (R_1, R_2)	$R_{total} = R_1 + R_2 = 150 \Omega$	$W_1:W_2 = R_1:R_2 = 2:1$
Parallel circuit (R_1, R_2)	$R_{total} = \frac{R_1 R_2}{R_1 + R_2}$ $= \frac{100}{3} \Omega$	$W_1 = \frac{V^2 t}{R_1}$, $W_2 = \frac{V^2 t}{R_2}$

Table 4-3. The parameters used in series and parallel circuit set into PHOTON.

Circuit	σ_1 ($S m^{-1}$)	σ_2 ($S m^{-1}$)	σ_{air} ($S m^{-1}$)	ϵ_1''	ϵ_2''	ϵ_{air}''	E_{rms} ($V m^{-1}$)
Only R_1	0.1 ($L=0.1m,$ $A=0.01m^2$)	-	-	-89877.42	-	-4.28×10^{-11}	1414.21
Series circuit (R_1, R_2)	0.05 ($L=0.05m,$ $A=0.01m^2$)	0.1 ($L=0.05m,$ $A=0.01m^2$)	4.76×10^{17}	-44938.71	-89877.42	-4.28×10^{-11}	1414.21
Parallel circuit (R_1, R_2)	0.2 ($L=0.1m,$ $A=0.05m^2$)	0.4 ($L=0.1m,$ $A=0.05m^2$)	4.76×10^{17}	-179754.84	-35909.70	-4.28×10^{-11}	1414.21

Table 4-4. The comparison of total work and heat generation for three conditions.

Circuit	W (J) (Joule's Law)	Q (J) (PHOTO software)
Only R_1	100	100.01
Series circuit (R_1, R_2)	$W_{total}= 66.67$ $W_1= 44.44, W_2= 22.22$	$Q_{total}= 66.67$ $Q_1=44.45, Q_2=44.45$
Parallel circuit (R_1, R_2)	$W_{total}= 300$ $W_1= 100, W_2= 200$	$Q_{total}= 300.03$ $Q_1= 100.03, Q_2= 200$

4.4 Results and discussion

In this study, the temperature distribution of four typical filling patterns were simulated and compared with experimental results to investigate the effect of arrangement of different components during ohmic heating. The amount of heat generation inside samples varies in relation to the distribution of electric field.

Based on estimated heat generation, the temperature of four filling patterns were predicted by the governing heat transfer equation. The temperature distributions of experiment and modeling in center horizontal cross section undergoing ohmic heating processing at four situations are listed in Fig. 4-4, Fig. 4-9, Fig. 4-14 and Fig. 4-19. It turned out that three-dimensional models for predicting temperature distribution of all the filling patterns during ohmic heating were generally in good agreement with experimental data. At the beginning, temperature distributions showed the consistent trend with the final temperature distributions showed in Fig. 4-8, Fig. 4-13, Fig. 4-18 and Fig. 4-23, respectively. The temperature difference appeared in the beginning of modeling because of the difference in electric field distribution by the different arrangement of mashed potato and mashed potato with 1 wt % sodium chloride. With the time expending, the difference became more and more noteworthy, resulted in significance difference of temperature distribution in all filling patterns at the end of ohmic heating. Simulations suggest the presence of significant hot and cold zones, implying the need

of further optimization of cell and electrode design for more uniform heating. In particular, solid composite food system, which has many components with different thermal properties, needs much more concern.

The measured temperatures in the middle area on the horizontal cross section were higher than the simulated temperatures, which may be caused by varying instantaneous voltage applied.

And electric conductivity difference which may occur using different measuring method (by water bath and undergoing ohmic heating) also may cause the experiment results slightly higher than prediction. Moreover, the current interference for thermocouple is considered to be another reason for this kind of error. This phenomenon was more obvious at the location where heat generation was high. The time lapse with the action of taking out from cavity and section cutting between end of heating and imaging could be considered as the reason for the temperature difference of thermography and temperature history measured by thermocouple (Pitchai *et al.*, 2012).

The experimental temperature histories of the specified points during heating were compared with the simulated result. Both of the experimental temperatures showed linear increasing, while all of them are slightly higher than the simulation. And the point 1 in series condition even showed the difference of over 8 °C at the end of heating. As the range of error (± 5 °C) of the temperature difference may also be observed between repetitive experiments, it was considered acceptable. The absorption of electric field power in the sample during simulation cannot be fully consistent with experiment, the slightly lower power absorption in the sample in simulation will lead to a weaker electric field intensity in the hot spot area and result in slower temperature increasing due to the lower electric conductivity used in models.

The filling patterns had a significant influence on temperature distribution in the same material. For example, as the mashed potato, the current density at the parallel situation was lower than that of series condition in which the materials arranged series and were perpendicular to the current direction (Fig. 4-4 and Fig. 4-9), resulting in localized under-treatment of food materials. We have noted the presence of a so-called “shadow area” of reduced electric field in the cross-sectional domain. In the same model, the temperature distribution was also different.

Fig. 4-14 showed the simulated temperature distributions inside pure-inside-salt model, the hot and cold spots both occurred in salted mashed potato. Compared with the simulation, the maximum temperature zone in the actual situation was much smaller, and so was the minimum temperature zone. Comparatively, at salt-inside-pure model, the hot areas happened in mashed potato (Fig. 4-19).

From the comparison of temperature histories of experiment and simulation during ohmic heating processing of parallel situation (Fig. 4-5 and Fig. 4-6), series situation (Fig. 4-10 and Fig. 4-11), pure-inside-salt model (Fig. 4-15 and Fig. 4-16) and salt-inside-pure model (Fig. 4-20 and Fig. 4-21), we can concluded that the heating rate of experiment was faster than that of experiment. At the end temperature, there was about 5 °C difference among all of the filling patterns. The location temperature of experimental and simulation along length and width were also compared (Fig. 4-7, Fig. 4-12, Fig. 4-17 and Fig. 4-22). The end temperature showed the same shape and similar value between them.

In modeling, the heat flux density also given as Fig. 4-24. Heat flux is a physical property of materials that indicates how fast heat travels through the material. Heat flux density is measured as the rate of energy transfer per given area in a given amount of time. In other word, if heat travels fast, then heat flux density is high, and vice versa. Form the result, not only the temperature distribution was dependent on the components with different properties and its arrangement but also the heat flux density.

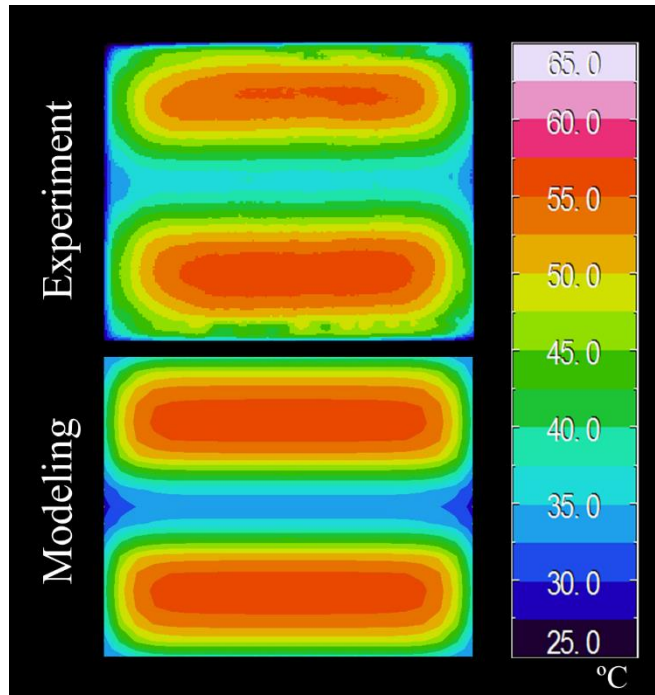


Fig. 4-4 Comparison of temperature distribution of experiment and modeling in center horizontal cross section undergoing 300 s ohmic heating processing of parallel situation.

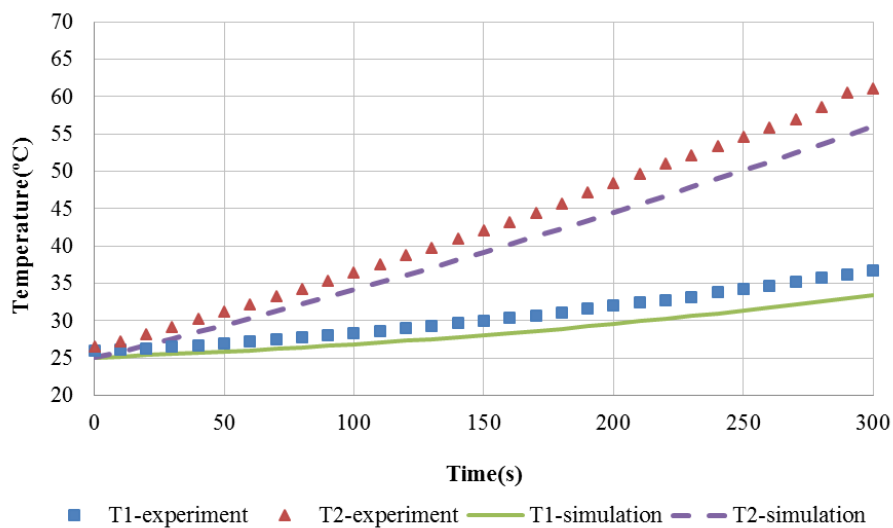


Fig. 4-5 Comparison of temperature history of experiment and simulation during ohmic heating processing of parallel situation (point 1 and point 2).

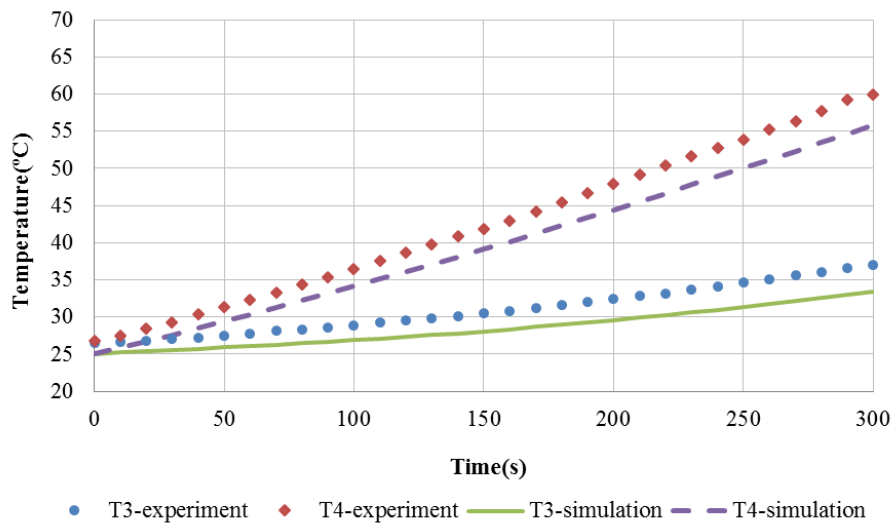


Fig. 4-6 Comparison of temperature history of experiment and simulation during ohmic heating processing of parallel situation (point 3 and point 4).

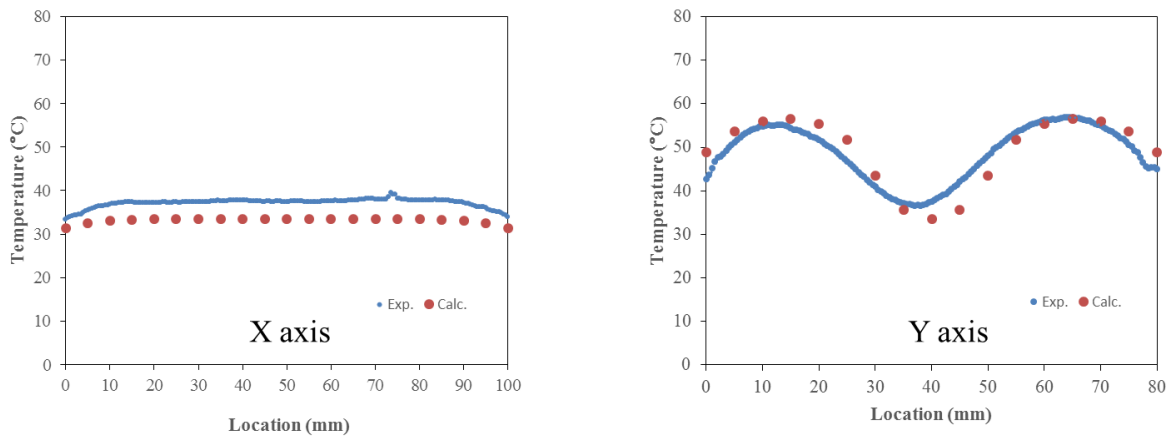


Fig. 4-7 Comparison of end temperature of experiment and simulation in center horizontal cross section undergoing 300 s ohmic heating processing of parallel situation.

left: along the length (X axis) at the center of width (Y=40 mm);
 right: along the width (Y axis) at center of length (X=50 mm)

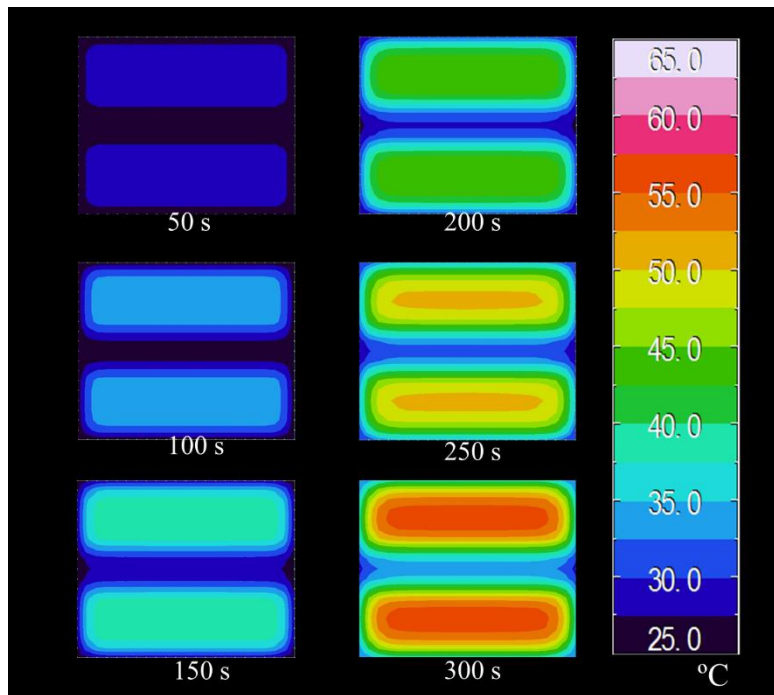


Fig. 4-8 The simulated temperature distribution of center horizontal cross section during ohmic heating processing of parallel situation (50 s, 100 s, 150 s, 200 s, 250 s, 300 s).

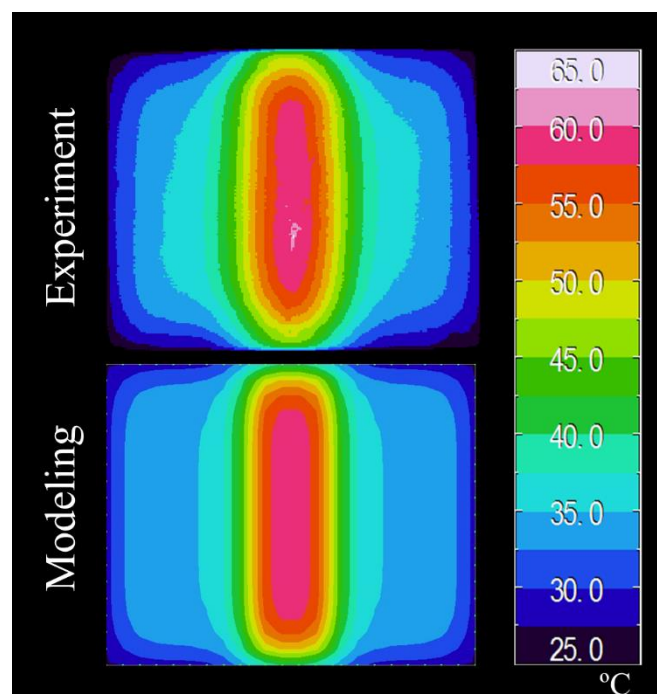


Fig. 4-9 Comparison of temperature distribution of experiment and modeling in center horizontal cross section undergoing 300 s ohmic heating processing of series situation.

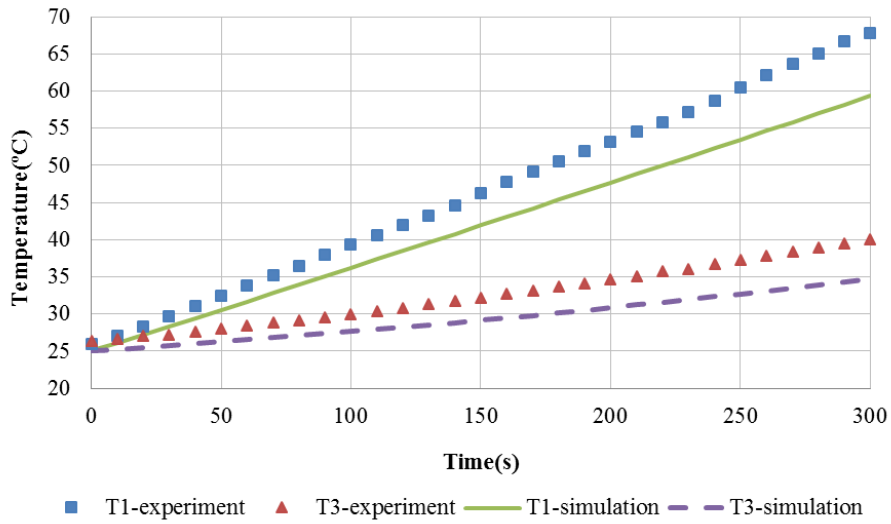


Fig. 4-10 Comparison of temperature history of experiment and simulation during ohmic heating processing of series situation (point 1 and point 3).

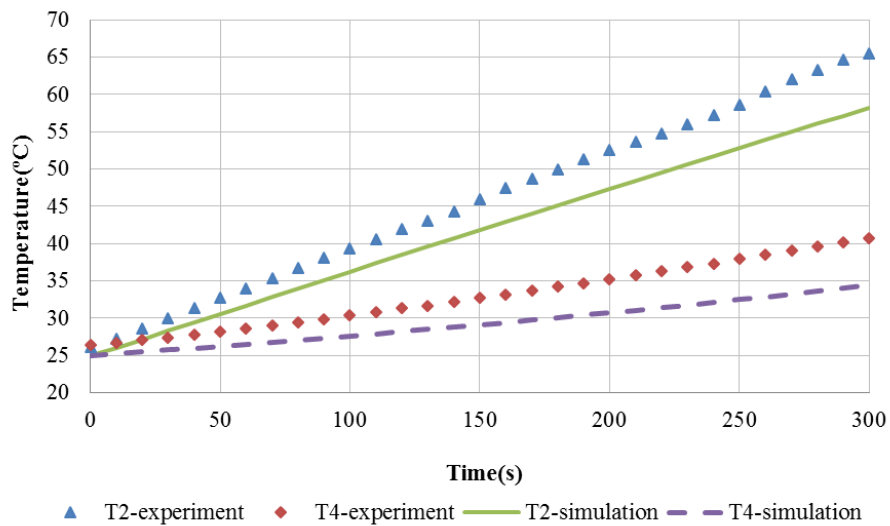


Fig. 4-11 Comparison of temperature history of experiment and simulation during ohmic heating processing of series situation (point 2 and point 4).

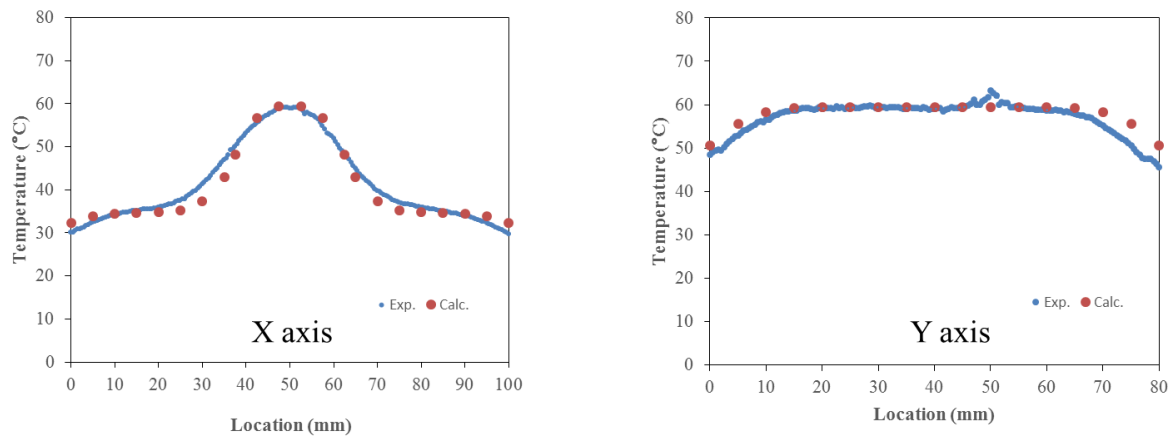


Fig. 4-12 Comparison of end temperature of experiment and simulation in center horizontal cross section undergoing 300 s ohmic heating processing of series situation.

left: along the length (X axis) at the center of width (Y=40 mm);

right: along the width (Y axis) at center of length (X=50 mm)

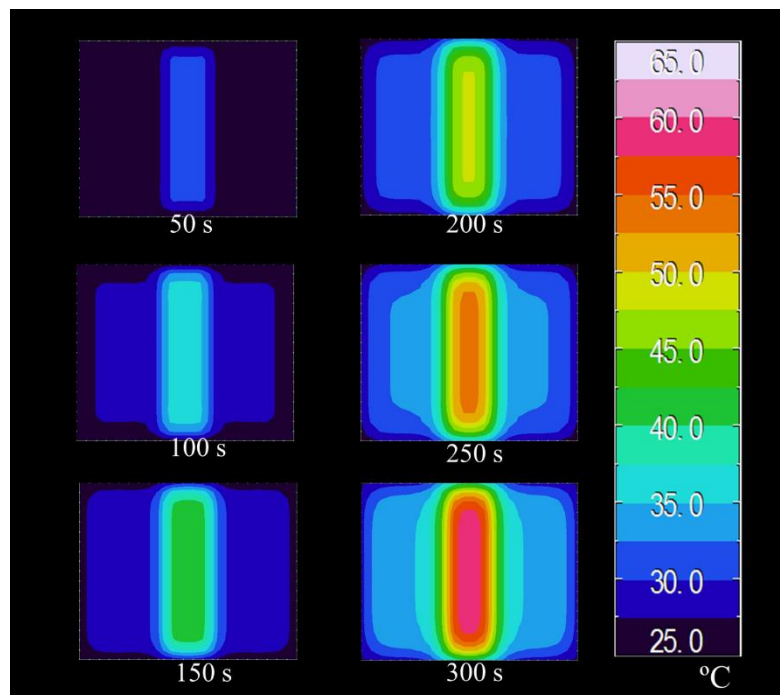


Fig. 4-13 The simulated temperature distribution of center horizontal cross section during ohmic heating processing of series situation (50 s, 100 s, 150 s, 200 s, 250 s, 300 s).

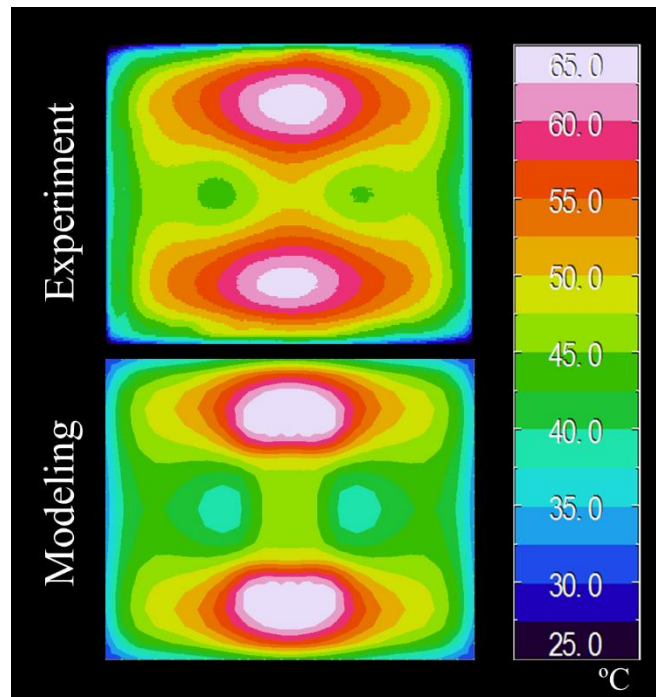


Fig. 4-14 Comparison of temperature distribution of experiment and modeling in center horizontal cross section undergoing 300s ohmic heating processing of pure-inside-salt situation.

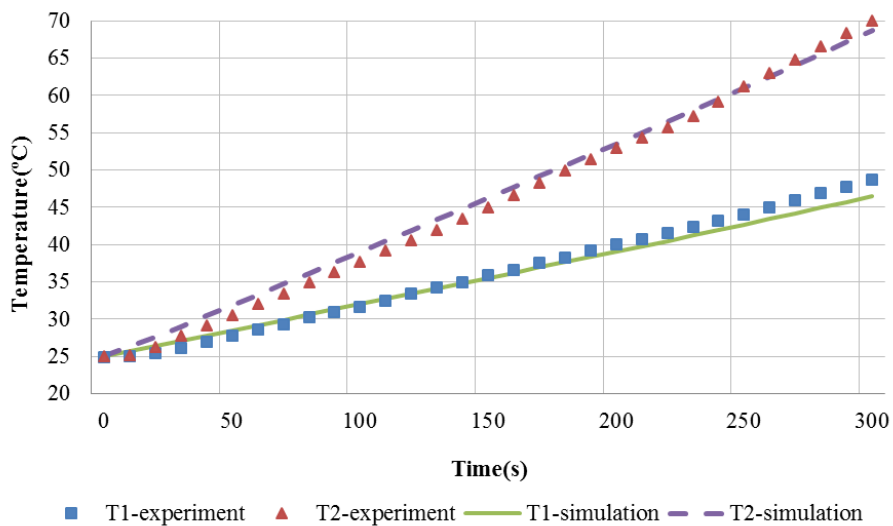


Fig. 4-15 Comparison of temperature history of experiment and simulation during ohmic heating processing of pure-inside-salt situation (point 1 and point 2).

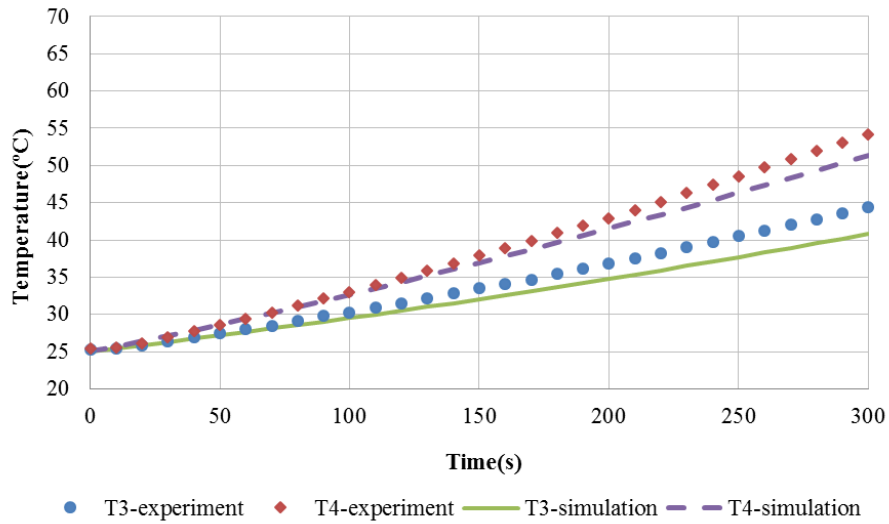


Fig. 4-16 Comparison of temperature history of experiment and simulation during ohmic heating processing of pure-inside-salt situation (point 3 and point 4).

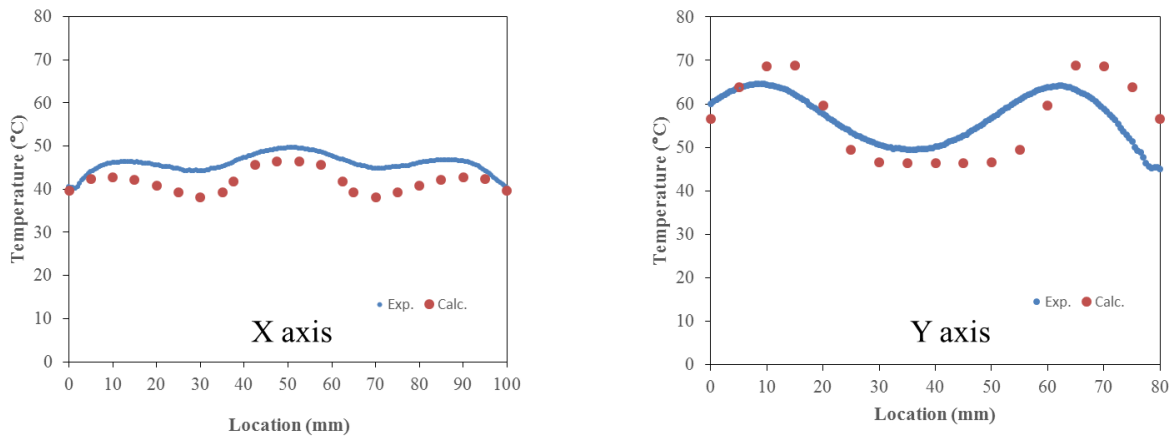


Fig. 4-17 Comparison of end temperature of experiment and simulation in center horizontal cross section undergoing 300 s ohmic heating processing of pure-inside-salt situation.

left: along the length (X axis) at the center of width (Y=40 mm) ;

right: along the width (Y axis) at center of length (X=50 mm)

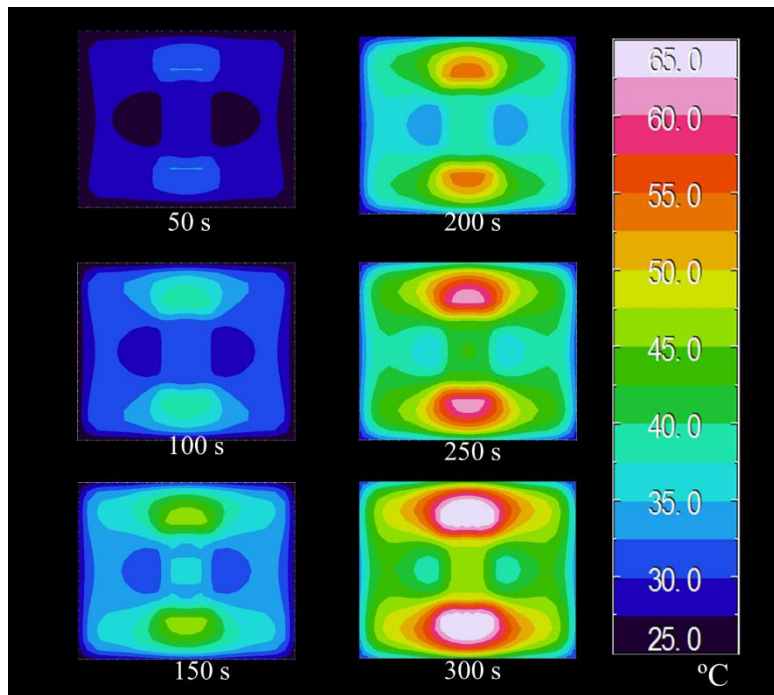


Fig. 4-18 The simulated temperature distribution of center horizontal cross section during ohmic heating processing of pure-inside-salt situation (50 s, 100 s, 150 s, 200 s, 250 s, 300 s).

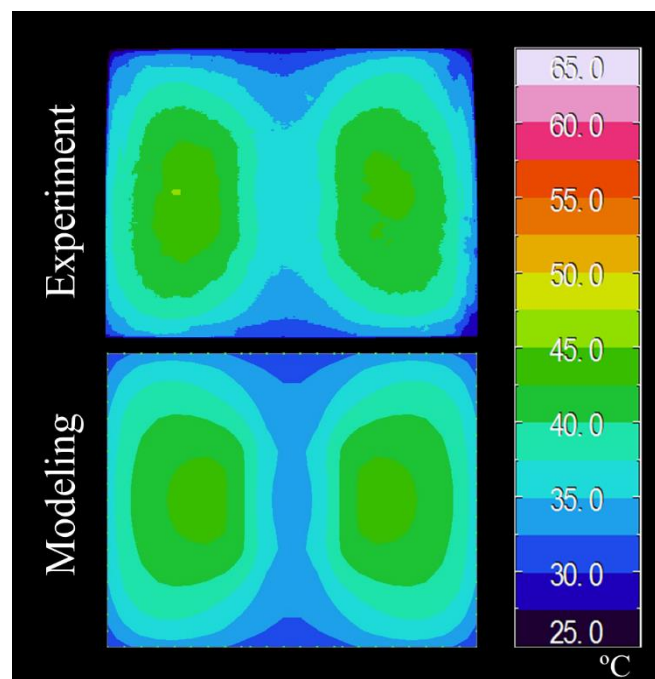


Fig. 4-19 Comparison of temperature distribution of experiment and modeling in center horizontal cross section undergoing 600 s ohmic heating processing of salt-inside-pure situation.

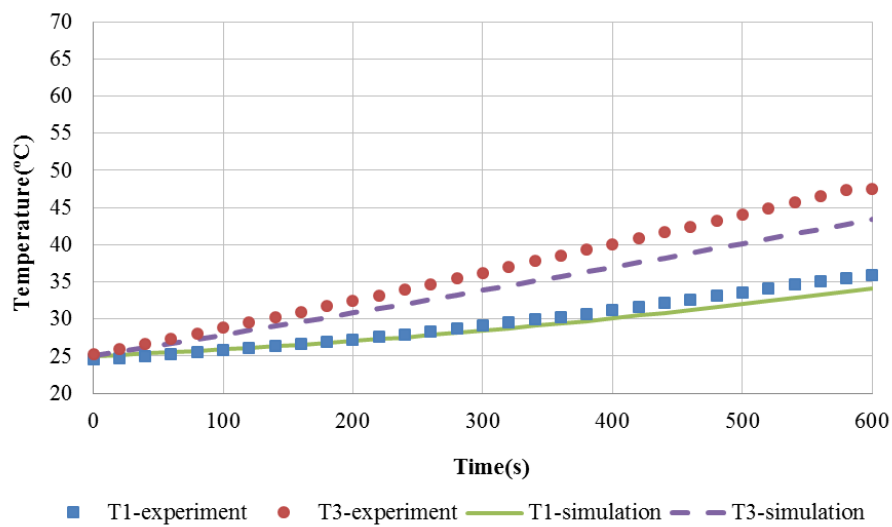


Fig. 4-20 Comparison of temperature history of experiment and simulation during ohmic heating processing of salt-inside-pure situation (point 1 and point 3).

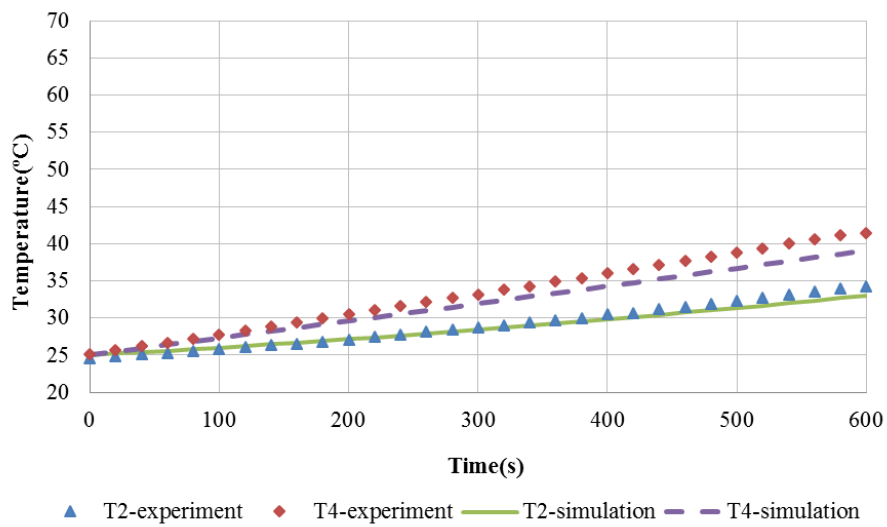


Fig. 4-21 Comparison of temperature history of experiment and simulation during ohmic heating processing of salt-inside-pure situation (point 2 and point 4).

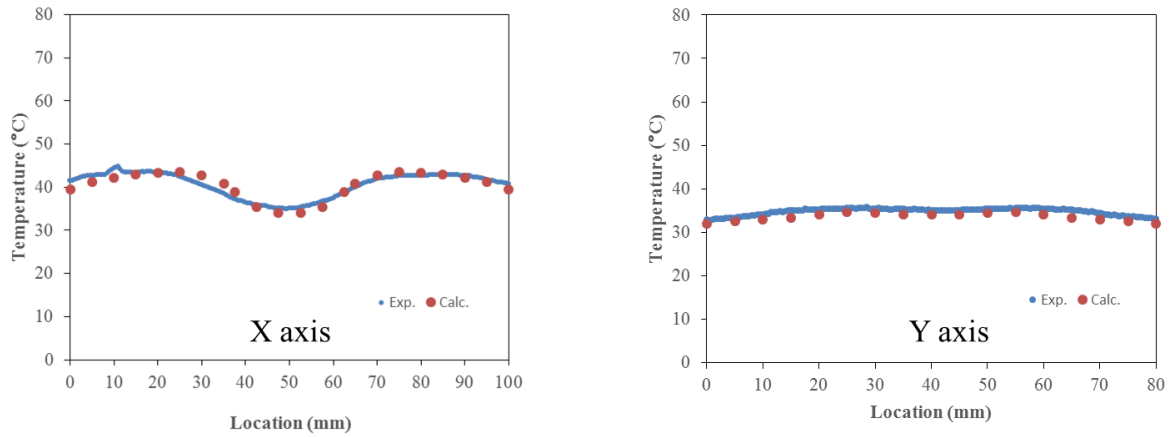


Fig. 4-22 Comparison of end temperature of experiment and simulation in center horizontal cross section undergoing 600s ohmic heating processing of series situation.

left: along the length (X axis) at the center of width (Y=40 mm);
 right: along the width (Y axis) at center of length (X=50 mm)

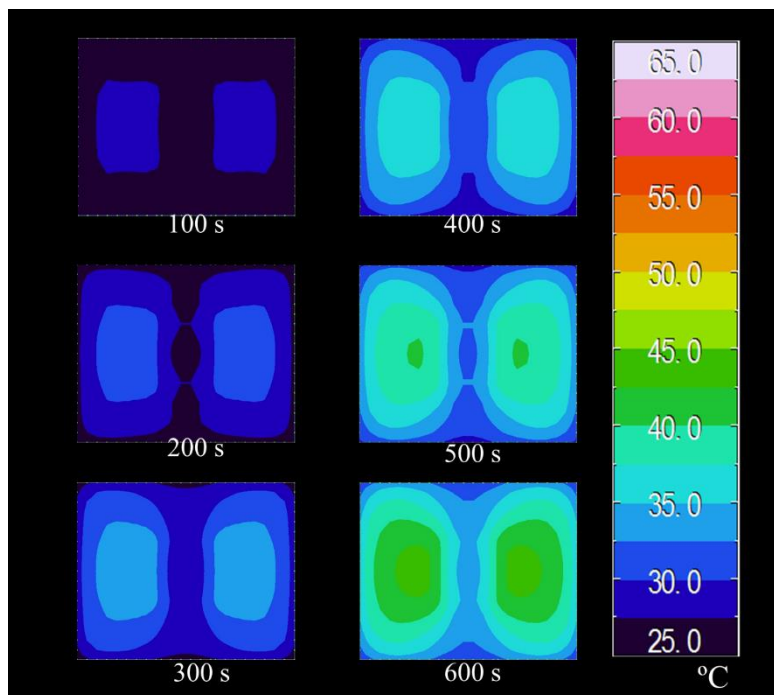


Fig. 4-23 The simulated temperature distribution of center horizontal cross section during ohmic heating processing of salt-inside-pure situation (100 s, 200 s, 300 s, 400 s, 500 s, 600 s).

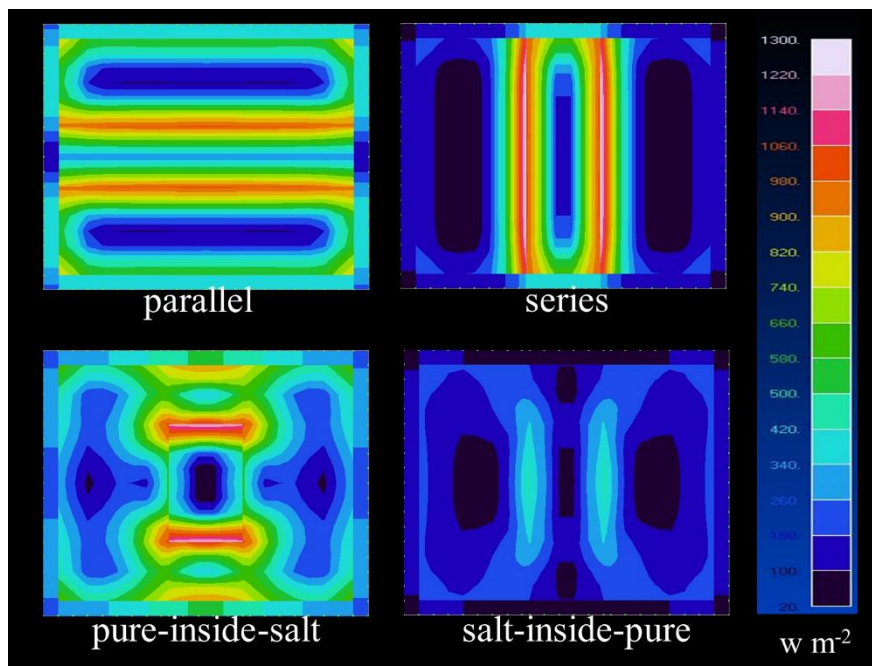


Fig. 4-24 The influence of heat flux density inside series model on temperature distribution of center horizontal cross section undergoing ohmic heating processing.

4.5 Conclusion

Temperature was estimated by coupling electromagnetic and heat transfer analysis using Maxwell's equation based on finite element method instead of Joule's Law, whereas the node coordinate and dielectric properties of sample were updated with time steps, and the heat generations were renewed according to these parameters. Three-dimensional model to predict the temperature distribution of solid composite food considering with the temperature dependency of electrical properties during ohmic heating that were consistent with experimental trends built confidence in model predictions, and pave the way for accurate simulation of specific situations.

The modeling explained the phenomenon of experiment from the theory view of the electrical field distribution. Otherwise, a good agreement showed between the modeling and experiment that implied a potential application for ohmic heating processing to get uniform temperature of solid composite food by electrode configurations. The new model showed a potential

application for optimizing ohmic heating processing to ensure safe pasteurization thermal process of solid composite food by electrode configurations (Fig. 4-25). The example model was pure-inside-salt model sized in 100 mm × 100 mm × 100 mm (mashed potato filling size is 30 mm × 30 mm × 100 mm inside), A was the simulation result after 300 s ohmic heating processing giving 50 V with a pair of electrode on one side all the time, B was also the simulation result of 300 s undergoing ohmic heating while the electrode changed the direction every 50 s. For this model, it was easy to conclude that the temperature distribution with electrode changing was more uniform than another one relatively. Further development of this model is required. Many physical or chemical changes during ohmic heating such as convection, evaporation, mass transfer and deformation are considered to be taken into account in real solid food with non-uniform properties in future studies.

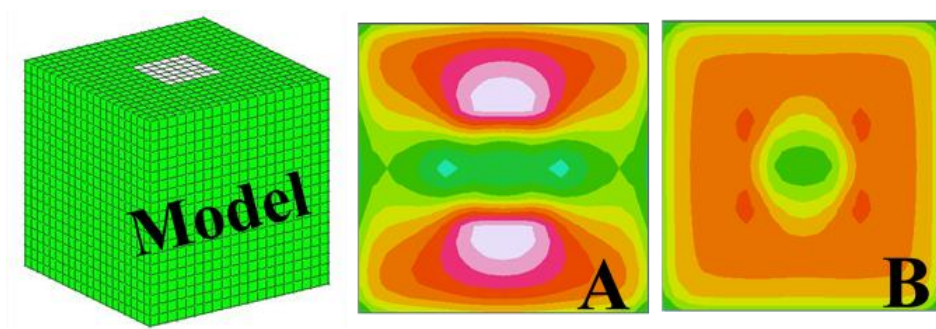


Fig. 4-25 The example model for optimizing ohmic heating processing of solid composite food by electrode configurations.

4.6 Reference

Birla, S. L., Wang, S., & Tang, J. (2008). Computer simulation of radio frequency heating of model fruit immersed in water. *Journal of Food Engineering*, 84 (2), 270-280.

Chandrasekaran S., Ramanathan S., & Basak T., (2011). Microwave material processing - a review. *AIChE Journal*, 58 (2), 330-363.

F. Marra., M. Zell., J.G. Lyng., D.J Morgan., D.A. Cronin. (2009). Analysis of heat transfer during ohmic processing of a solid food. *Journal of Food Engineering*, 91, 56-63.

- Gongyue Tang., Deguang Yan., Chun Yang., Haiqing Gong., Cheekiong Chai., Yeecheong Lam. (2007). Joule heating and its effects on electrokinetic transport of solutes in rectangular microchannels. *Sensors and Actuators A*, 139, 221-232.
- Knoerzer K., Regier M., & Schubert H., (2008). A computational model for calculating temperature distributions in microwave food applications. *Innovative Food Science and Emerging Technologies*. 9 (3), 374-384.
- Liu S., Fukuoka, M., & Sakai, N. (2013). A finite element model for simulating temperature distributions in rotating food during microwave heating. *Journal of Food Engineering*, 115 (1), 49-62.
- Markus Zell., James G. Lyng., Denis A. Cronin ., Desmond J. Morgan. (2009). Ohmic heating of meats: Electrical conductivities of whole meats and processed meat ingredients. *Meat Science*, 83, 563-570.
- Markus Zell., James G. Lyng., Denis A. Cronin ., Desmond J. Morgan. (2010). Ohmic heating of whole turkey meat- effect of rapid ohmic heating on selected product parameters. *Food Chemistry*, 120, 724-729.
- M. Shynkaryk., & S.K. Sastry. (2012). Simulation and optimization of the ohmic processing of highly viscous food product in chambers with sidewise parallel electrodes. *Journal of Food Engineering*, 110, 448-456.
- Oomori T. (1993). The foundation and application of microwave heating (pp. 52-54). *Electromagnetic Wave and Food*. Korin Publishing Company, Tokyo, Japan.
- S.M. Zhu., M.R. Zareifard., C.R. Chen., M. Marcotte.,S. Grabowski. (2010). Electrical conductivity of particle-mixtures in ohmic heating: Measurement and simulation. *Food Research International*, 43, 1666-1672.
- Soojin Jun., & Sudhir Sastry. (2007). Reusable pouch development for long term space mission: a 3D ohmic model for verification of sterilization efficacy. *Journal of Food Engineering*, 80, 1199-1205.
- Whitaker, S. (1977). *Fundamental Principles of Heat Transfer* (pp. 215). Robert E. Krieger Publishing Company, Malabar, FL, USA.

W.-R Fu., & C.-C Hsieh. (1999). Simulation and verification of two-dimensional ohmic heating in static system. *Journal of Food Science*, 64 (6), 946-949.

Xiaofei Ye., Roger Ruan., Paul Chen., Christopher Doona. (2004). Simulation and verification of ohmic heating in static heater using MRI temperature mapping. *Lebensm.-Wiss. u.-Technol*, 37, 49-58.

Chapter 5- Conclusions and future work

My research underlined the importance of considerations of understanding, characterizing and modeling of temperature distribution in solid composite food during ohmic heating. In this study, the mashed potato and mashed potato with 1 wt % sodium chloride (water content of both are 80 wt %) were used as the different pseudo food ingredients whose electric characteristics differed. And the electric conductivity, which is the important parameter used for temperature analysis and modeling, has been investigated using a LCR meter considering temperature dependency. Temperature distributions of four typical filling patterns with ingredients of non-uniform electric properties were investigated during ohmic heating. And a three-dimensional finite element computational model was also successfully established for estimating the temperature changing of solid food by coupling the analysis of electrical heat generation and heat transfer. Simulated temperature distributions on cross-sections were finally verified by experimental ones which were taken by an infrared thermal camera.

In my study, the electric conductivities of mashed potato and salted mashed potato showed temperature and frequency dependency and salt concentration also influenced. We found out the relationships between them and the empirical equations were given. Furthermore, different ingredients and their arrangement conditions in the container were observed to have a significant influence on the temperature distribution during ohmic heating. Good agreements have been found between simulations and experimental results.

As well known, in ohmic processing, the product is heated volumetrically by dissipation of electrical current, passing through the food, into heat. The rate of heating is directly proportional to the square of the electric field strength and the electrical conductivity. Ohmic heating is an emerging technology with large number of actual and future application. The possibilities for ohmic heating includes blanching, evaporation, dehydration, fermentation, extraction, sterilization and pasteurization.

So far, the applications of ohmic heating for the thermal processing have not been widespread. One of the obstacle is that the calculations of changing product temperature for the ohmic heating process are quite complicated and not completely studied. The quality of ohmically-heated food product is another aspect that requires further studies. Nonetheless, the information regarding the comparison between the qualities of ohmically-heated and conventionally-heated products in the case of heating them at the same levels of temperature and time are required so

that the effect of ohmic heating mechanism on the product quality will be clarified. Still more research is needed to completely understand all the effects produced by ohmic heating. The effects of the applied electric field, the incident electric current and different microorganisms and foods still need to be more deeply studied.

Also more research is required addressing cold-spots identification and measurement during complex foods processing especially multiphase foods. Studies on modeling, prediction and determination of the heating pattern of complex foods are also required to assist on the design of food sterilization or pasteurization processes and for successful development of a final product package that enables the application of ohmic heating.

Nomenclature

Latin letters

f	frequency (Hz)
k	thermal conductivity ($\text{W m}^{-1} \text{K}^{-1}$)
t	time (s)
A	cross sectional area (m^2)
B	magnetic induction (Wb m^{-2})
C_p	specific heat ($\text{J kg}^{-1} \text{K}^{-1}$)
D	electric displacement (C m^{-2})
E	electric field intensity (V m^{-1})
E_{rms}	root mean square value of the electric field (V m^{-1})
H	magnetic field (A m^{-1})
I	current (A)
J	current density (A m^{-2})
L	length between electrodes (m)
P	power (W)
Q	internal volumetric heat generation term ($\text{J s}^{-1} \text{m}^{-3}$)
Q_{gen}	heat generation due to ohmic effect ($\text{J s}^{-1} \text{m}^{-3}$)
R	resistance (Ω)
T	temperature ($^{\circ}\text{C}$)
V	voltage (V)
W	electrical work (J)
X	reactance (Ω)

Greek symbol

ε	complex permittivity
ε_0	permittivity of free space 8.854×10^{-12} (F m^{-1})
ε''	relative dielectric loss factor

μ	permeability (H m^{-1})
ρ	density (kg m^{-3})
ρ_m	electric volumetric charge density (As m^{-3})
σ	electric conductivity (S m^{-1})
ω	angular frequency (rad s^{-1})

Subscripts

<i>m</i>	multimeter
<i>Exp.</i>	experiment
<i>Calc.</i>	calculated

Acknowledgements

First of all, I would like to extend my sincere gratitude to my supervisor Prof. Noboru Sakai, Laboratory of food thermal processing, Tokyo University of Marine Science and Technology, for his instructive advice and useful suggestions on my thesis and experiment. He has walked me through all the stages of the writing of this thesis. Secondly, my high tribute shall be paid to Prof. Mika Fukuoka, Laboratory of food thermal processing, Tokyo University of Marine Science and Technology, without her consistent and illuminating instruction, this thesis could never reach its present form. I also gratefully acknowledge the help of Prof. Yu-dong Cheng, headmaster of Shanghai Ocean University, who led me into the world of food science and technology, and has taught me a lot even after I left Shanghai.

I owe a special debt of gratitude to Ph.D Shi-xiong Liu, my senior, who has given me patient instructions and great help during the experiment. I also owe much to all the members of Laboratory of food thermal processing for their valuable suggestions and critiques which are of help and importance in my research, especially Moe Higo, my tutor.

Also, I want to express my gratitude to Japan-China-Korea Exchange Project Promotion Committee and Tokyo University of Marine Science and Technology and Shanghai Ocean University, for providing me this precious opportunity to study in Japan, and supporting me both in living and research.

Last but not the least, my gratitude also extends to my family who have been assisting, supporting and caring for me all of my life.